POLITECNICO DI TORINO

Master's Degree in Communications and Computer Networks Engineering

Master's Degree Thesis

Enhancements of EEG Artifact Automatic Correction Algorithm and Processing of Hemiplegic Patients' EEG

Supervisors

Prof. Roberto GARELLO

Prof.ssa Gabriella OLMO

Prof. Vito DE FEO

Candidate

Cristina DEL PRETE

April 2023

Abstract

Patients suffering from severe brain injuries may experience the unfortunate condition of being conscious, but unable to interact or communicate with the outside world. In these cases, the lack of communication does not allow doctors to have a complete understanding of patients' state of consciousness leading to misdiagnosis compromising the choice of the best treatment. The use of Brain-Computer Interface (BCI) is a promising strategy to analyse brain signals and evaluate the presence of consciousness.

The proposed project aims at realizing a low-cost non-invasive BCI able to detect and distinguish consciousness states through the use of electroencephalographic (EEG) and electromyographic (EMG) signals. We initially recorded from healthy subjects to train our algorithm. The method involves a pre-processing part, entirely realized on MATLAB, to clean the raw EEG signals and obtain Readiness Potentials (RP), a special type of Event Related Potentials (ERP), giving a measure of the intentionality behind motion. Machine learning algorithms are successively devoted to the classification of the movement between voluntary, semi-voluntary and involuntary with the extraction of peculiar RP features.

After an introduction on consciousness and its states, the brain anatomy and the recording methods, this thesis will focus on enhancing the pre-processing algorithm devoted to the automatic correction of EEG artifacts. In particular, it will be discussed (1) the different artifacts affecting the EEG signal; (2) the use of Independent Component Analysis (ICA) to detect and correct them in frequency and time domain; (3) the analysis of different detrending method to remove slow drifts; (3) the improvements obtained on the RPs.

We recorded EEG and EMG also from hemiplegic patients asking them to perform or imagine to perform a motor task. The application of the pre-precessing chain to these signals will be discussed to prove the presence of intention and motor programming exploiting Lateralized Readiness Potentials (LRP).

Table of Contents

List of Tables

List of Figures

Acronyms

BCI
Brain-Computer Interface

BP
Bereitschaftspotential

BSS
Blind Source Separation

CMA
Correct Motor Asymmetry

CNS
Central Nervous System

CNS
Cerebrospinal Fluid

EEG
Electroencephalography

EMG
Electromyography

EOG
Electrooculography

ERP
Event Related Potential

GNW

Global Neuronal Workspace

IC

Independent Component

ICA

Independent Component Analysis

IIT

Integrated Information Theory

LIS

Locked-In Syndrome

LPR

Lateralized Readiness Potential

MCS

Minimally Conscious State

MRCP

Motor Related Cortical Potential

MP

Motor Potential

MUAP

Motor Unit Action Potential

MUAPT

Motor Unit Action Potential Train

NCC

Neuronal Correlates of Consciousness

PCI

Perturbational Complexity Index

PMP

Pre-Motion Positivity

PNS

Peripheral Nervous System

RP

Readiness Potential

SNR

Signal-to-Noise Ratio

VS

Vegetative State

TMS

Transcranial Magnetic Stimulation

Chapter 1

Consciousness

What is consciousness? Is it related to the body? How? The answers to these questions have been matter of controversy between philosophers from the earliest days and they are still importantly related to morality and free will topics.
In this chapter, different concepts of "consciousness" and the two main theories of mind will be introduced; then, the neuroscience point of view will be discussed through the Neuronal Correlates of Consciousness (NCC); lastly, the levels of consciousness and related disorders will be described.

1.1 Definition and theories of consciousness

The term "consciousness" derives from the Latin verb *conscire* composed by *con-* «with» and *scire* «to know»; probably, a loan-translation of the Greek word *synedeisis* [1]. It is commonly defined as the ability to know and perceive [2] or the state of being awake, thinking, knowing and understanding what is happening around us [3].

The concept of consciousness has been notoriously discussed by philosophers over the centuries: they have been trying to define what allows human being to be conscious and whether this ability is intrinsic with the body or not. From Plato to Freud, the discourse has brought to two main theories: Dualism and Materialism.

The Western philosophers Plato and Aristotle can be considered as the precursors of Dualism since they recognized the distinction between body and soul. However, it is only with René Descartes that the mind-body problem became a central topic. In his arguments, Descartes sustained that the body is a material thing with a measurable extent and sensitive to the laws of physics; on the other hand, the mind is immaterial, lacking of spatial extension and not measurable. The distinction of these two substances raised many objections against Descartes. In fact, he tried to

explain that the concurrence of feelings and physical events was due to a structure in our brain where mind and body could interact, but this was not enough to convince Materialists.

Materialism claimed that everything existing is made of matter and, consequently, that mental and brain states are identical and can be proved scientifically. Following this idea, more radical theories were proposed, but the attempts of giving satisfying demonstrations became more complex than expected. The relationship between brain and phenomenal properties was, and still is, difficult to understand since one can be present without the other. The problem of explaining the connection between specific conscious and brain states in a fulfilling way is unique and Joseph Levine summarized it in the expression "the explanatory gap". Similarly, David Chalmers articulated the phrase "the hard problem of consciousness" to identify the difficulty of explaining the physical processes giving rise to the subjective feelings and sensations of conscious experiences, also known as *qualia*. On the other hand, Chalmers defined "easy problems" the ones relating more with the functions of consciousness: the ability to discriminate and categorize stimuli, the ability of a cognitive system to access its own internal states and the difference between wakefulness and sleep. Therefore, also Materialists missed something to explain consciousness.
Neuroscience started playing a key role to provide some answers and, in the end, it merged with philosophy into a single study called neurophilosophy which is still working to solve the mystery behind consciousness.

1.2 Neurological point of view

Neuroscientists define consciousness as everything we experience, but they recognize that brain's complexity and conditioning do not allow a logical argumentation for a full explanation. Putting aside the philosophers' question of why we have particular feelings, they focus on the scientific exploration of Neuronal Correlates of Consciousness (NCC), i.e. the minimal neuronal activity mostly correlated with the presence of consciousness [4].
It is possible to distinguish different aspects involving conscious experiences:

- *level of vigilance*, the state of attention needed to live psychic activities in contact with ourselves and the surrounding environment;
- *peripheral correlates of consciousness*, corresponding to the modification occurring with the different levels of vigilance;
- *electrical brain activity*, expressing the functional level of the cerebral cortex through dedicated instruments;

- *contents of consciousness*, related to all the mental activities as perceptions, feelings and thoughts occupying our mind on a given moment;
- *self memory*, meaning the continuous comparison between the sensorial inputs, personal past experiences and perception of oneself identity implicating a given behaviour;
- *selective attention*, defined as the mental concentration and focus on a given content.

These characteristics can be associated to different parts of the thalamocortical system, composed by the cerebral cortex and the thalamus, whose interactions are necessary to generate the processes corresponding to conscious scenes.[5]

1.2.1 Theories of consciousness

The two most popular theories of consciousness in neuroscientific world are the **Global Neuronal Workspace** theory (GNW) and the **Integrated Information Theory**(IIT). Both recognize two properties of consciousness:

- **Integration**. Every conscious experience, independently from its content, consists of a single and independent "scene". It is also private and unique, since it is experienced from a particular point of view which cannot be shared.
- **Differentiation**. A given conscious state implies an extremely rapid selection among a collection of different states large as much as one's experience and imagination, and it may lead to different thoughts or actions. [6]

GNW, by Bernard J. Baars and others, observes that being conscious of something implies that many parts of the brain have access to that information, while the localization of specific motor system implies unconsciousness. Therefore, GNW states that consciousness arise when sensory information is broadcast globally to multiple systems processing the data.[4]

IIT, developed by Giulio Tononi *et al.*, considers the experience as intrinsic, structured, specific-distinct, unified and definite. Consequently, any complex and interconnected mechanism able to encode cause-effect relationships will have a level of consciousness, provided that it does not lack of integration and complexity. In other words, consciousness is the intrinsic causal power associated with complex systems as human brain. IIT also provides a measure of consciousness through a single non-negative number Φ: if $\Phi = 0$ the system is not conscious; the higher Φ, the more intrinsic causal power the system possesses and the more conscious it is. Human brain has a high specific connectivity which implies high Φ and then very

high level of consciousness.[4]
The emphasis on integrated information and complexity as hallmarks of consciousness is well seen by many researchers that developed new theories starting from it.

1.3 Levels of consciousness

A normal state of consciousness is composed by:

- phenomenal consciousness, or *arousal*, referring to the state of alertness or wakefulness and clinically corresponding to the spontaneous eye opening;

- focal consciousness, or *awareness*, describing the subjective experience and deducted by the ability to follow commands [7].

Given these aspect, it is possible to represent every level of conscious experience in a two-dimensional space (Figure 1.1). However, under some conditions, it is not possible to asses an individual's level of consciousness. New researches starting from the IIT, designed an empirical measure of brain complexity, called the **Perturbational Complexity Index** (PCI). It measures the amount of information in the integrated response of the thalamocortical system to a perturbation and it was used to discriminate levels of consciousness between healthy subjects and brain injured patients. The analysis involved recordings of transcranial magnetic stimulation (TMS) evoked potentials and obtained promising results.

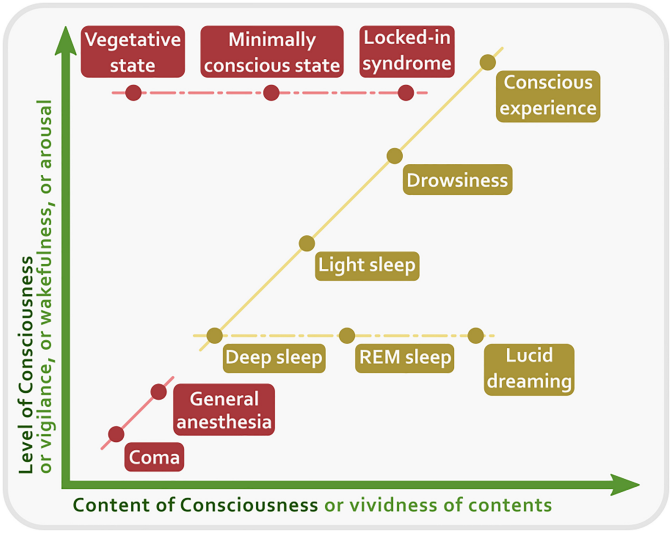

Figure 1.1: Two-dimensional representation of different level of consciousness. The vividness of the experience is represented on the X axis; the wakefulness, vigilance or arousal are represented by the Y axis. Red indicates the clinical conditions; yellow the normal physiological states. Taken from [8].

1.3.1 Disorders of consciousness

As previously mentioned, some conditions do not allow to determine the presence of consciousness and its level. This is what happens to brain injured patients. While some may completely lose their brain functions, i.e. incur in brain death, those surviving may rapidly recover from coma or go through different states of consciousness before getting back. Others, instead, may remain in one of these states depending on the damaged structure.

The disorders of consciousness that can occur are:

- **Coma**: the acute state during which patients are neither aroused nor aware; the eyes are constantly closed and not manifesting voluntary responses. There are changes in the control and regulation of basic vital functions. This state cannot last longer than 4 weeks, but it depends on the patient's medical condition and age. Recovering from coma may lead to vegetative state, minimally conscious state or, rarely, locked-in syndrome.

- **Vegetative State (VS)**: clinical condition which may occur after coma; it is characterized by the absence of consciousness and responsiveness, a sufficient preservation of neurovegetative functions and motor reflex, and normal sleep-wake cycle. Patients in vegetative state give no signs of self-consciousness or

awareness of the environment and can not communicate with others. However, there is a motor response to pain, but not a voluntary avoidance, and cranial nerves and spinal reflexes are preserved.

- **Minimal Conscious State (MCS)**: condition in which patients are aroused and manifest self or environment awareness through minimal behaviours. The behavioural responses of a patient in MCS are inconsistent, but reproducible and they can be sustained long enough to be differentiated from reflexes. MCS can occur after coma or be the evolution of a previous vegetative state; it can last a short period or for a more or less indefinite time until the patient's death.

Locked-In Syndrome (LIS) is not a disorder of consciousness, but a state of awareness and vigilance with the concurrent condition of quadriplegia and paralysis of lower cranial nerves. Patients with *classical* LIS can communicate by blinking or through vertical eye movement; in case of *incomplete* or *total* LIS, ocular movements are difficult or totally absent. [9] [10] [11]

Chapter 2

The brain

The brain is the most important organ in the human body, but it is also the most complex. Each part is specialized in important functions as body control or interpretation of informations received from the outside.
In this chapter, the main components of the brain and their role will be presented to have a better idea of how disease and injuries can affect it.

2.1 The anatomy of the brain

The human nervous system is composed by two parts:

- the **Central Nervous System** (CNS), which analyses the received informations and generates appropriate answers;
- the **Peripheral Nervous System** (PNS), perceiving inside and outside stimuli and transmitting the answers elaborated from the CNS.

The CNS includes brain and spinal cord which are both protected by the skull and meninges, i.e. three layers of tissue called *Dura Mater*, *Arachnoid* and *Pia Mater*. Moreover, a watery substance called Cerebrospinal Fluid (CNS) cushion from injuries, washes out waste and impurities, and delivers nutrients.[12][13]
The brain is composed by three parts: cerebrum, cerebellum and brainstem.

Cerebrum

The cerebrum is the largest part of the brain and it is divided into two major parts, right and left hemispheres. The two are separated by the great longitudinal fissure, but connected by the *corpus callosum* which delivers messages from one half to the other. The surface of the cerebrum consists in a grey matter layer called cerebral cortex. It is possible to identify four functional sections for each hemisphere:

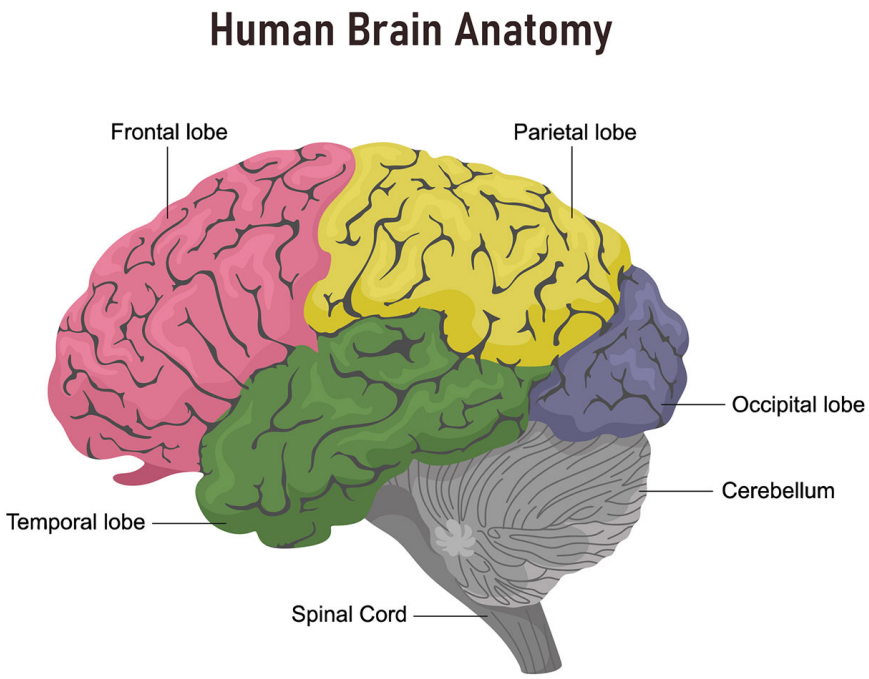

Figure 2.1: Brain anatomy. The brain is composed by three parts: cerebrum, cerebellum and brainstem. Each hemisphere of the cerebrum can be divided in four lobes. Taken from [12]

- **Frontal lobe**: located in the front of the head, it is the largest lobe and it is responsible for intellectual and behavioural functions, and for speech and motor ability; in particular, the areas planning voluntary movements are located in the premotor area, while those producing movements in the primary motor cortex.

- **Parietal lobe**: it is the middle section of the brain processing sensory information to identify objects and understand spatial relationships; it is also involved in pain and touch interpretation.

- **Temporal lobe**: located at the side of the hemisphere, it is involved in visual and verbal memory, and its backside enables the interpretation of other people's emotions and reactions.

- **Occipital lobe**: the back part of the brain involved in processing visual informations as colours and shapes received from the retinas of the eyes.

Damages to these lobes affect their functions.[14][13][15]

The cerebral cortex communicates through white matter with deeper parts usually responsible of essential behaviour for survival. In particular:

- the *thalamus*, consisting of two symmetrical egg-shaped masses, is located above the brainstem with neurons radiating out through the cerebral cortex; it serves as relay station for almost all the informations that come and go to the cortex transmitting messages to the appropriate areas;
- the *pituitary gland*, a small gland located at the base of the brain behind the nose, controls other endocrine glands in the body;
- the *hypothalamus*, a small structure at the base of the brain near the pituitary gland, handles informations from autonomic nervous system and controls hunger, emotions, temperature regulation, and circadian rhythms;
- the *amygdala*, a cluster of nuclei located close to the base of the brain, is involved in functions including memory, emotion, and the body's fight-or-flight response;
- the *hippocampus*, a structure located in the temporal lobe, is important in memory, learning and in the control of emotional responses;
- the *pineal gland*, located behind the third ventricle, helps regulate the body's internal clock and circadian rhythms with the secretion of melatonin.[12][13][15]

Cerebellum

The cerebellum is the second largest part of the brain. It has an ovoid structure weighting 130 g–140 g and located beneath the posterior occipital lobes, behind the brainstem. It has left and right hemispheres connected by the *vermis* and an interior central tissue, called *arbor vitae*, spreading branches and sub-branches through the hemispheres. The cerebellum has the primary function of maintaining posture and balance by controlling the tone of muscles and limbs' position, but it also fine-tunes movements.[12][16]

Brainstem

The brainstem is the lower extension of the brain in front of the cerebellum and connecting the spinal cord. It consists of three structures: *medulla oblongata*, *pons* and *midbrain*. It passes messages between the various part of the body and the cerebral cortex, but, more importantly, it controls involuntary functions as respiration, digestion, circulation and reflexes.[12][14]

2.2 Neurons and glial cells

Neurons are the fundamental unit of the nervous system. A neuron consists in three parts:

- **soma**, containing nucleus and cytoplasm;
- **dendrites**, small extensions of the soma acting as antennas picking messages from other neurons;
- **axons**, extended structures specialized in the transmission of the information through synapsis.

It is possible to classify neurons as:

- *primary sensitive neurons*, if they transmit the information from sensorial parts to the nervous system;
- *motor neurons*, if they transmit information from the nervous system through synapsis with muscles;
- *interneurons*, neurons transmitting to other neurons.

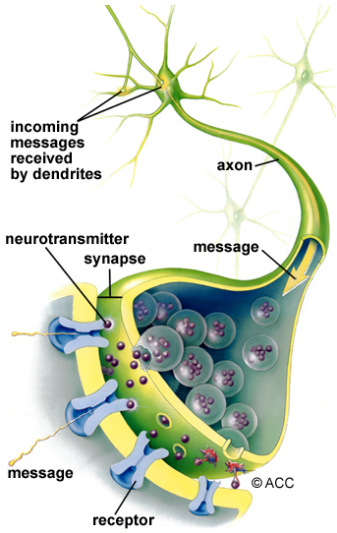

Figure 2.2: Neuron's structure and signal transmission. The incoming messages from dendrites travels along the axon and are transmitted to other neurons through synapsis.[13] Taken from [15]

Glia cells are non-neuronal cells outnumbering neurons by about 50 to one. They sustain the nervous system and its processes through nourishment, protection and

structural support. Indeed, they form a barrier protecting the brain and the spinal cord against chemical substances coming from blood. Moreover, they contribute to neuronal communication and neurochemical signal transmission.[15][17]

2.2.1 Neurons electrical activity

Neurons generate two types of electrical signals:

- **action potentials**, discrete voltage spikes propagating along the axon to its terminals and essential for cell-cell communication;

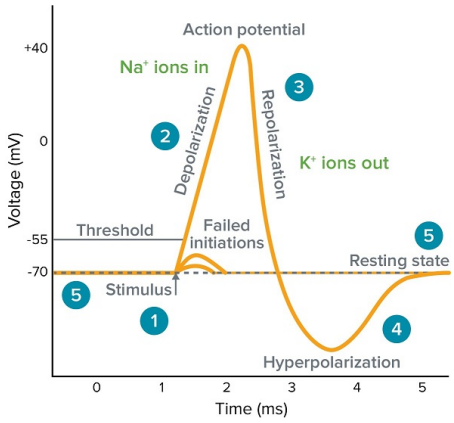

Figure 2.3: Action potential passing a point on a cell membrane. The resting membrane potential is $-70\,\text{mV}$. If the stimulus increases the potential above the threshold, it keeps increasing and sodium ions enter. When the peak is reached, potassium ions exits with a repolarization. Before going back to the resting state, the membrane potential hyperpolarizes for a small period. Taken from [18]

- **postsynaptic potentials**, voltages arising when neurotransmitters bind to receptors and are able to initiate (excitatory postsynaptic potentials) or inhibit (inhibitory postsynaptic potentials) action potentials.

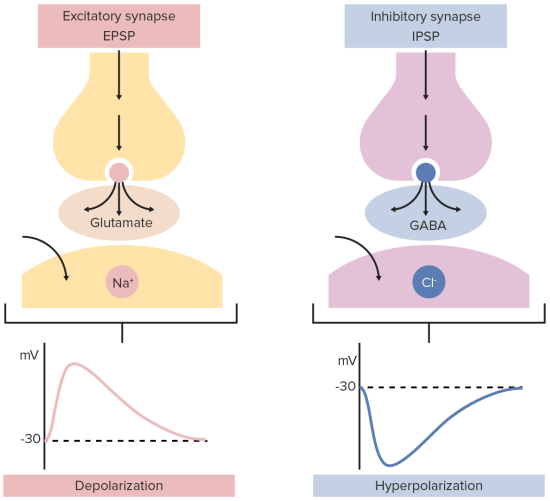

Figure 2.4: Postsynaptic potentials can be: excitatory (left), the presynaptic terminal releases glutamate which allows depolarization of the membrane with positive ions (Na+); inhibitory (right), the release of GABA causes the entrance negative ions (Cl-) and the hyperpolarization of the membrane. Taken from [19]

While action potentials last 1 ms and can be measured with a microelectrode into the brain in an *in vivo* recording, this is not possible with postsynaptic potentials even if they can last tens or hundreds of milliseconds. Postsynaptic potentials are mainly generated by pyramidal cells, the main type of neuron in the cerebral cortex. When an excitatory neurotransmitter is released from presynaptic terminals in apical dendrite, it causes an electrical current (positive ions flow) from the extracellular space into the cell and a negative voltage outside the apical dendrites; the current flows through the neuron exiting in the region of the cell body and the basal dendrites (Figure 2.5). The dipole created by this process on a single neuron can not be measured with scalp electrodes; however, if neurons receives the same input and have the same orientation, the summation of dipoles will make possible recording local field potential.[20]

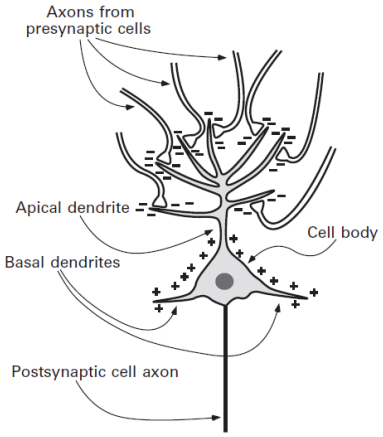

Figure 2.5: Scheme of neurotransmission in a pyramidal cell. An excitatory neurotransmitter released from presynaptic cells in apical dendrites causes the positive ion flow inside the postsynaptic neuron and negative on the outside region. The positive current flows through the neuron exiting in the cell body region and basal dendrites. Taken from [20]

Chapter 3

Biosignals and Readiness Potentials

As previously said, consciousness is still a mystery and a challenging topic especially in neuroscientific research. The actual assessment of a patient's state of consciousness is based on attitudes and responses which can be voluntary or not. Consequently, the possibility of having inaccurate diagnosis or misdiagnosis is large and depends on the severity of brain injuries. The integration of neurofunctional imaging to behavioural assessment can overcome these limitations and make the detection of consciousness in non-responsive patients more accurate.
In this thesis, it is presented a project conducted in collaboration with the University of Essex and aiming at the implementation of a non-invasive Brain Computer Interface(BCI) allowing the user to send neuronal commands to a controller interpreting and classifying motor actions. The high correlation between consciousness and intention of voluntary movements, whether performed or imagined, has been studied through Event Related Potentials (ERP), voltages arising in the brain consequently to a specific stimulus or event.
This chapter focuses on the relation between awareness and motor intention, the biosignals and the particular type of ERP, called Readiness Potentials, essentials for this project.

3.1 Conscious intention and motor cognition

As largely demonstrated in neuroscience, consciousness is closely related the concepts of free will and motor intention, whether the action is performed or just imagined. Conscious experience requires awareness of one's own actions and their ability to control them. However, it is important to make some distinction between some concepts:

- *Movement's intention*: the decision and urge to move;
- *Consciousness of the intention:* the awareness of wanting to move;
- *Consciousness of the in progress motion*: the knowledge of moving;
- *Consciousness of completing the programmed movement*: the awareness that the action has been performed as wanted.

Motor consciousness requires the sense of agency through one's body. Many researches focused on the individuation of specific brain areas determining the conscious experience leading to action's fulfilment. Patrick Haggard, professor of neuroscience at the University College London, studied the conscious intention and motor cognition. He concluded that any voluntary movement requires unaware motor preparation preceding the decision of take action, i.e. the conscious intention. Consciousness of motor intention activates the front pre-supplementary motor area (SMA) and, then, it is independent from the movement execution. Indeed, damages to the motor cortex can cause paralysis, while injuries to premotor areas generates more complex deficits in motor cognition altering awareness and intentionality. Movement awareness is then strictly related to the motor preparation stages.
Blakemore, Wolpert and Frith developed a model reflecting the sequence of events producing and controlling the motor execution (3.1). The basic blocks composing the model are:

- **Motor planning**: it generates the motor commands necessary to compute the desired state comparing it with the actual state; then, it creates two copies of the motor sequence: one for the motor cortex and the other for the predictor block;
- **Prediction model**: it estimates the sensory consequences (predicted state) of the programmed action before performing the movement.
- **Comparator A**: it compares the predicted state with the desired state; if the two coincide then the subject gets the perception of performing the action, the so-called "sense of agency", before execution;
- **Comparator B**: it compares the implemented state, i.e. after movement, with the desired state; if they coincide, the subject is aware that the movement has been performed.

This model highlights the link between conscious intention and motor cognition to program the movement and to be aware of the effects produced in the external environment.[21][22]

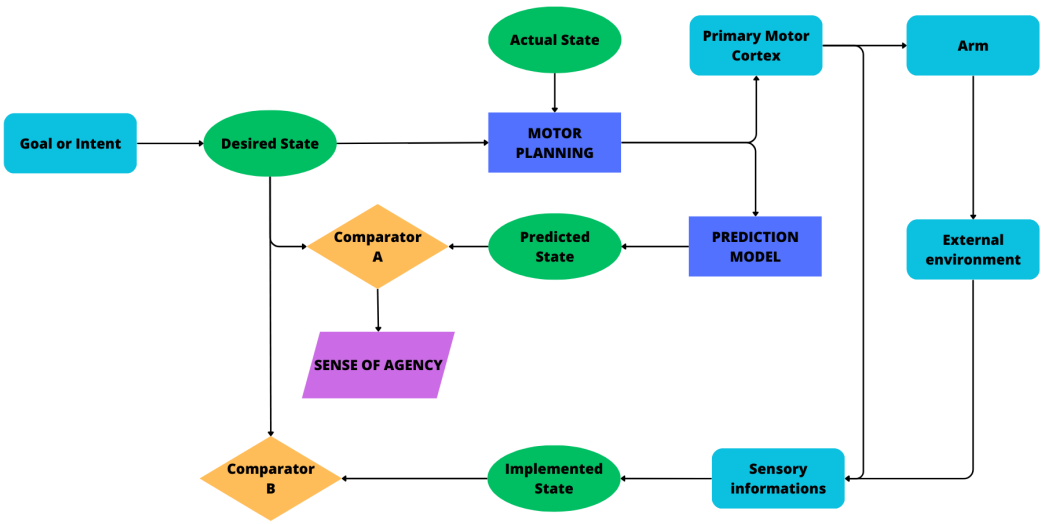

Figure 3.1: Computational framework for action.

Important studies by Berti *et al.* demonstrated that damages to the comparator B lead to disorders as *anosognosia for hemiplegia*, a transient condition in which patients are partially paralysed and claim to be able to move with the paralysed parts of their body. In this cases, the motor intention and planning prediction are preserved, which means that their sense of agency is generated correctly, but the comparison computed between implemented state and desired state is not correct.[23]

3.2 Biosignals: Electroencephalogram and Electromyogram

The two fundamental biosignals for this project are electroencephalogram (EEG) and electromyogram (EMG) signals. In the following, their generation, characteristics in time and frequency domain, and recording method are briefly presented.

3.2.1 Electroencephalogram signal

Electroencephalography is a technique to acquire brain potentials reflecting the human cognitive behaviour. It was discovered by Hans Berger (1924) who proved through different experiments that the synchronous activity of cortical pyramidal neurons can be registered by applying electrodes on the scalp and amplifying the

signal. The device used to acquire the cortical activity is the electroencephalogram and it includes electrodes, conductive gel, amplifiers and Analog-to-Digital converters. Electrodes are placed on the scalp with a small quantity of conductive gel according to the International 10-20 system which positions adjacent electrodes at a distance equal to the 10% or 20% of the total front-back (*naison-inion*) or left-right (ears) distance(3.2).

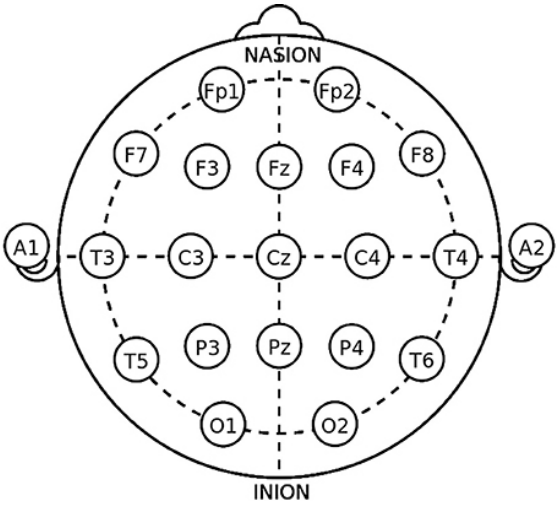

Figure 3.2: International 10-20 system. Taken from [24]

Each electrode is labelled with letters indicating the lobe (Fp–Pre-Frontal, F–Frontal, C–Central, P–Parietal, O–Occipital, T–Temporal) and numbers referring to the hemisphere (odd–left, even–right and "z" for the central line). EEG waveforms have amplitude between 10 µV and 500 µV and they can be distinguished by their morphology, topography, symmetry and synchronism. In frequency, EEG spectrum ranges between 0.1 Hz–100 Hz and it can be divided in different bands associated to different behaviours and brain's state:

- *Delta waves (0.1 Hz–4 Hz)*: characterized by the highest amplitude due to the strong synchronization of neurons generating cortical potentials; typical of deep sleep, infants and patients in comatose state;

- *Theta waves (4 Hz–8 Hz)*: related to subconscious activity, they occur during deep relaxation and meditation; frequent in children under 13 years old and abnormal in adults;

- *Alpha waves (8 Hz–13 Hz)*: they normally occur in adults while relaxing; they act as a bridge between conscious and subconscious state;

- *Beta waves (13 Hz–30 Hz)*: related to conscious actions and thinking; they occur while talking, solving problems, judging and making decision and all other activities requiring attention and concentration;

- *Gamma waves (30 Hz–100 Hz)*: related to perception and full awareness; usual while integrating sensory experiences and memory.

3.2.2 Electromyogram signal

Electromyography is the technique used to measure muscle response after nerve's stimulation through an instrument called electromyograph. Muscles in resting state do not produce electric signals; while, when a stimulus occurs, a brief and wide signal can be registered.
EMG recordings can be obtained by voluntary or stimulated contraction: the first produce a random signal, while the second a deterministic signal.

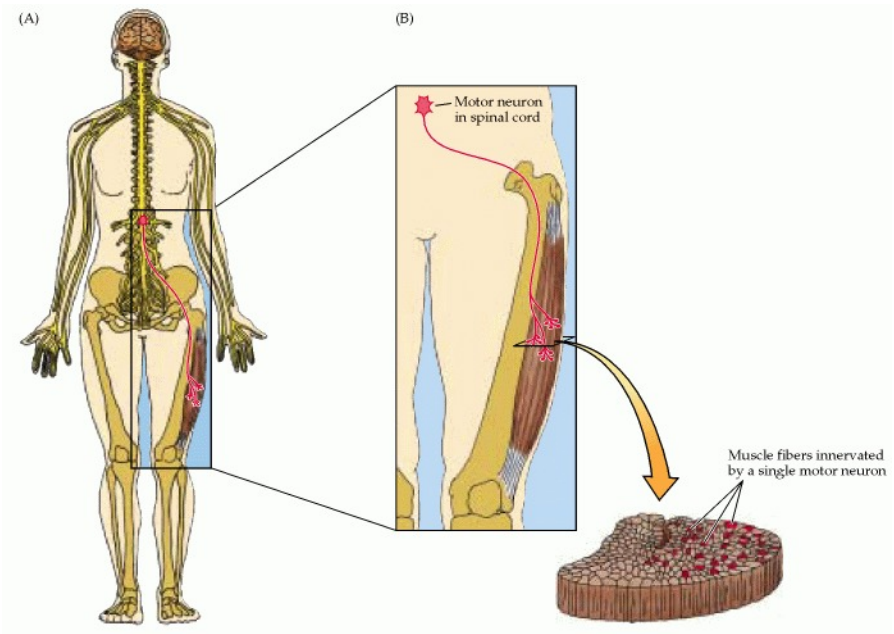

Figure 3.3: Motor Unit: the set of motor unit and muscle fibers. Taken from [25]

The set of alpha motor neuron and muscle fibers forms the **Motor Unit**(3.3), considered the muscle's functional unit. The axons departed from the spinal cord propagate action potentials activating the muscle fibers; their post-synaptic membrane is depolarized and then it produces different waveforms. The summation of the action potentials is called **Motor Unit Action Potential** (MUAP).

Different motor units in the same area influence the signal detected by an electrode; then, it will record the summation of a MUAPs' sequence, also called MUAPT (Motor Unit Action Potential Train). Being non synchronous, this summation generates interference, therefore, filtering is necessary to obtain the final EMG signal.
EMG can be recorded in two ways:

- Surface EMG, non invasive techniques using two or more electrodes recording the muscle activity from the surface above the muscle or skin. At least two electrodes are needed because the final signal is given by the difference between them.

- Intramuscular EMG, a more invasive technique recording signals from the inside with needle electrodes and a reference surface electrode.

3.3 Readiness Potentials

ERPs reflect the summed activity of postsynaptic potentials produced by various type of events each characterized by a particular waveform.[26] ERPs occurring in temporal relation with movements are Motor Related Cortical Potentials (MRCP) and they can be obtained from EEG and EMG recordings during repetitive movements: the EMG gives time onsets to identify EEG traces that, averaged, gives the MRCP. In 1965, Kornhuber and Deecke analysed MRCPs and identified three main components:

- Readiness Potential (RP) or Bereitschaftspotential (BP), strictly related to the motor intention;

- Pre-Motion Positivity (PMP), the predominant component over the hemisphere ipsilateral to the motion side;

- Motor Potential (MP), corresponding to the movement site.

RPs are characterized by a slow negative potential preceding the motion onset of 2 s which can be divided in: *early component* ($\sim 1.5\,\mathrm{s} - 0.4\,\mathrm{s}$ prior to onset), the slow but gradual increase in negativity, symmetrical between the two hemispheres, attributed to the supplementary motor area and premotor cortex; *late component* ($\sim 0.4\,\mathrm{s} - 0\,\mathrm{s}$ before the onset), generated by the primary motor cortex.[27] The amplitude and spatial focus of the RP depends on many particulars of the task as preparatory states, motor intention, limb dominance, free movement selection, rate of movement repetition or perceived effort.[28]

3.3.1 Lateralized Readiness Potential

The Lateralized Readiness Potential (LPR) enhances the RP's characteristic of having larger amplitudes on the hemisphere controlateral to the side of the muscle contraction, before the onset of the unilateral motor response. Kutas and Donchin hypothesised that the beginning of lateralized activation corresponds to the moment when the subject decides the side to move, i.e. the conscious intention to move appears.

The most used method to obtain LPR is the **Double Subtraction Method**, designed by De Jong (1988). It defines the motor asymmetry as the potential difference between two opposite sites of the scalp due to lateralization and it requires the RPs obtained performing the same task with right and left side:

1. the first difference is computed between the RPs of C3 and C4 channels for both tasks;
$$(RP_{C3} - RP_{C4})_R \qquad (RP_{C3} - RP_{C4})_L \tag{3.1}$$

2. the second subtraction consists in the difference between the first amplitude difference for the right side task and the left side and it is called **Correct Motor Asymmetry** (CMA).
$$CMA = (RP_{C3} - RP_{C4})_R - (RP_{C3} - RP_{C4})_L \tag{3.2}$$

The second subtraction allows the elimination of the contribution due to the hemispheres' asymmetry and the CMA parameter indicates the extent of lateralization. Several studies proved that the CMA can be obtained also during motor imagery and differs only in the action execution. Rosembaum and Kornblum (1982) elaborated the Motor Priming Paradigm in which participants are subject to two stimulus: the first provides information on particular aspects of the movement; the second is to execute the motor task. It has been observed the rising of cortical negativity in the controlateral side during the interval between the two stimuli which indicates that the motor preparation is specific to the response, even if the movement is just imagined.[29]

3.3.2 Libet's Experiment

In 1983, Benjamin Libet and his associated conducted a series of experiments to understand whether the conscious awareness of voluntary intention to act appears at the same advance timing of Readiness Potentials. The participants to this experiment were asked to repeatedly perform a simple movement, as flexing a finger, in a spontaneous way while EEG and EMG signals were recorded. Moreover, watching a clock rotating, they had to note the time at which they felt the urge to

move (W time). Libet obtained an average of conscious intention time of 206 ms before muscle contraction, a long time after RP onset, suggesting that the brain prepares to act over a large period before the subject's conscious willing. Libet recognized then three distinguished moment in the RP: the conscious decision to move (W), the unconscious brain event preparing the action (C) and the muscle movement (M).[21][30][31]

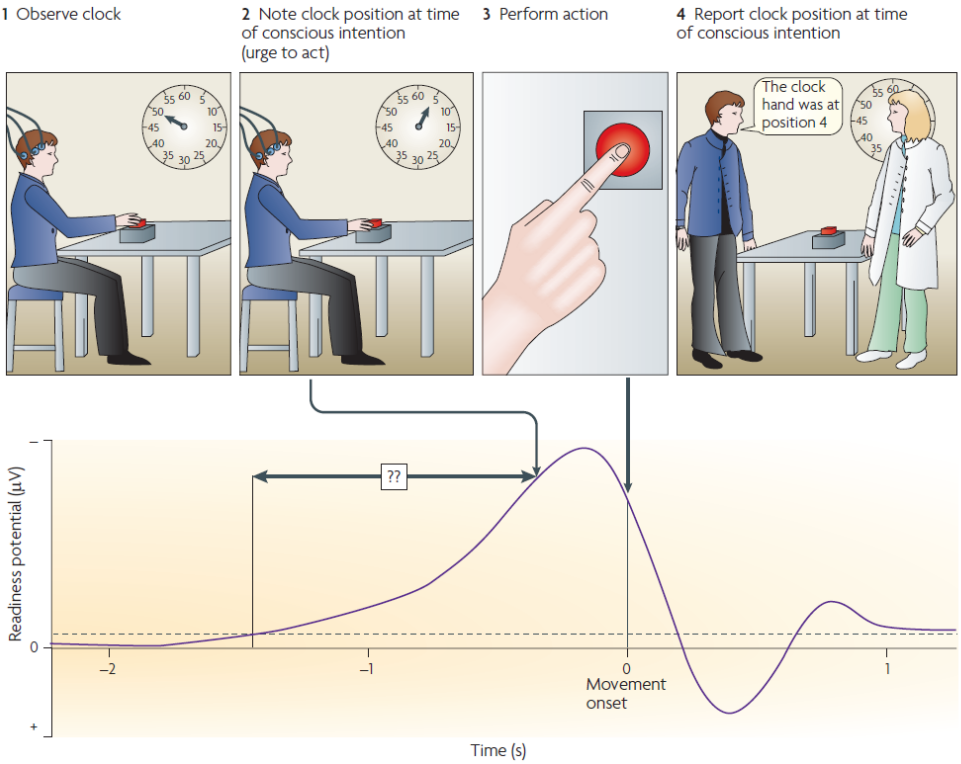

Figure 3.4: Libet experiment and Related Potential. Taken from [30]

Chapter 4

Readiness Potentials recording

The essential biosignals for this project were recorded in Turin at *Centro Puzzle* from male and female healthy volunteers and patients affected with hemiplegia, aged between 18 and 65 years.
The signals were recorded and displayed on screen through the software *Galileo NT*.
The type of biosignals recorded are:

- **Electroencephalography (EEG) signals**, acquired using an EEG cap with a varying number of passive Ag/AgCl electrodes according to the adopted protocol;

- **Electromyography (EMG) signals**, recorded with several adhesive electrodes attached to areas of the muscles to contract;

- **Electrooculography (EOG) signals**, acquired by placing two adhesive electrodes above and below each eye.

Figure 4.1: Experimental setup.

4.1 Tasks and Protocol

Different protocols have been adopted over the years, each requiring different type of tasks and experimental setups.

4.1.1 2012 - 2015 Protocol

A clock timer is displayed on the computer and the subject flexes the index finger of the right hand every 10 s for 6 min. In this way are obtained 40 epochs to use for the ERP evaluation. More alternative tests were performed:

- *Using the mouse*: the movement is obtained by clicking the mouse button;
- *Using both hands*: the subject is asked to use both hands; the experimenter indicates which hand to use every time;
- *Short trials*: the movement is performed every 5 s to validate the hypothesis of lack of free will;
- *Bimanual*: the subject uses both hands at the same time.

4.1.2 2015 - 2018 Protocol

The subject observes a clock projection on a screen and he/she is asked to repeat a simple movement every 10 s for 6 min and 40 s. The movements can be: flexing

the index finger, voluntary movement of foot or leg, the coordinated movement of hand and leg, the patellar reflex of the knee. Some subjects were blindfolded and they performed the tasks under indication of an operator.

4.1.3 2018 Protocol

The volunteers perform three tasks:

- *Voluntary task*: the subject moves the index finger in a time window of 10 s–13 s after a sound. In this way, the subject has the opportunity to make voluntary choice.
- *Semi-voluntary task*: the index finger movement must be performed as soon as the subject hears the beep.
- *Involuntary task*: the patellar reflex is stimulated through a gavel by an operator, but the subject does not hear the beep sound, then the moment of the stimulus can not be predicted.

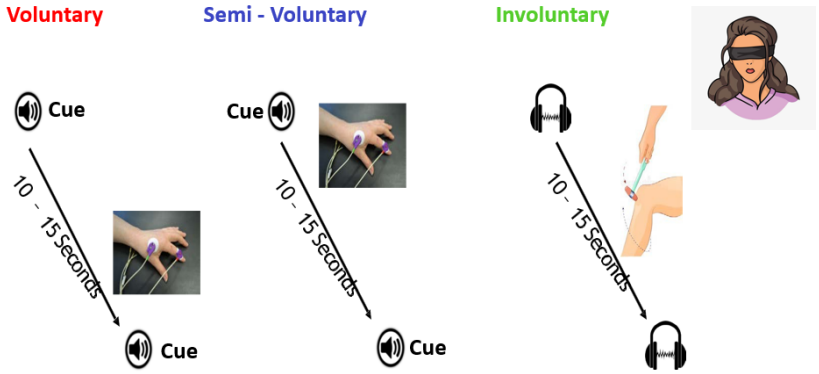

Figure 4.2: 2018 Protocol tasks.

4.1.4 Dataset classification

The acquired data have been classified according to the subject information, the type and mode of acquisition, and the instrumentation used. In this protocol, the use of Labjack, i.e. a USB based measurement and automation device providing digital input/output, allows the triggering for the movement while connected to a Data Acquisition System (DAQ). The recordings' classification involved the evaluation of Labjack and EMG signals' quality on a scale ranging from 0 to 3

depending on the variability of the signal and the noise.

Each dataset has been named with a string of 45 characters composed by:

- **8 characters** anonymizing the subject's informations with the first letter of the name, the first letter of the surname, the last digit of the recording year, the last two digits of the year of birth, the month of registration and 0/1 depending whether the subject is male or female;
- **5 characters** identifying the type of EEG electrode mounting: 32C18 stands for 32 channels, while OBE12 for the bridge electrodes;
- **4 characters** for the protocol used: A18C for 2018 protocol, B18C for 2015-2018 protocol and VOPC meaning Very Old Protocol (2012-2015 protocol);
- **3 characters** describing the condition of the subject between blindfolded (FOL) and not (UNF);
- **5 characters** identifying the type of task performed: voluntary (VOL18), semivoluntary (SEM18) or involuntary (INV18);
- **4 characters** classifying the task: right forefinger (RFOF), left forefinger (LFOF), bimanual forefinger (BFOF), mouse click with the right hand (RMOU), right leg (RLEG), left leg (LLEG), right foot (RFOO), left foot (LFOO), right hand and leg (RHLE), left hand and leg (LHLE);
- **4 characters** indicating the channel used for the EMG: EMG1 for channel 1, EMG2 for channel 2 and EMGX for channel without number;
- **4 characters** to classify the quality for the EMG and Labjack indicated respectively by E and L followed by 0/1/2/3.

4.2 Experimental setup

The recording of has been performed through the following instrumentation:

- **Data Acquisition device**: Galileo Suite, EB Neuro with Brain Explorer amplifiers;
- **Galileo Software** processing and displaying the EEG traces;
- **Stimulation system**: Labjack and OpenSesame software for the acoustic signal;
- **Synchronization system**: Labjack and photocoupler circuit;

- **Recording tools**: EEG cap, adhesive electrodes (4 for EOG signal and 2 for EMG signal), ground electrode for EMG (on the wrist for voluntary and semi-voluntary tasks, on the ankle for involuntary) and two earlobes reference electrodes for EEG;

- **Additional accessories**: conductive paste TEN20, abrasive paste NUPREP, conductive EEG gel, a syringe with a blunt needle.

The subject sits on a raised chair which avoid the feet from touching the floor. In one computer, it must be installed the software OpenSesame for starting the task and emitting the acoustic signal. Another computer with the Galileo software must be connected with the EEG cap and it allows to visualize, process and export the signal. The subject is seated behind the first computer and on his left side.

The electrodes' positioning starts from EMG and EOG sensors; then, earlobes and wrist (or ankle) electrodes are mounted, using TEN20. Subsequently, the EEG cap is set positioning Cz electrode in the middle between *naison*, *inion* and the two earlobes. The skin is cleaned from sebum and dead cells with the abrasive paste NUPREP and then the cap is filled with conductive gel with the blunt needle to improve the signal conduction and improve the adhesion with the skin.

4.3 Software

The biosignals acquired are made compatible with the Matlab environment to go under a signal processing improving the quality and eliminate disturbing elements which could affect the classification.

The elaboration of Event Related Potentials exploits the EEGLAB toolbox with a particular plug-in called MRCPLAB, created for this project.

4.3.1 EEGLAB

EEGLAB is an interactive Matlab toolbox developed by Swartz Center for Computational Neuroscience (SCCN). It is used to process continuous and event related EEG, MEG and other electrophysiological signals. Its graphic interface (GUI) permits the selection between different operations in time and frequency domain. EEGLAB also offers modelling and visualization method for event-related brain dynamics. Being an open-source platform, research programmers can share new method with the publication of new plug-in functions.

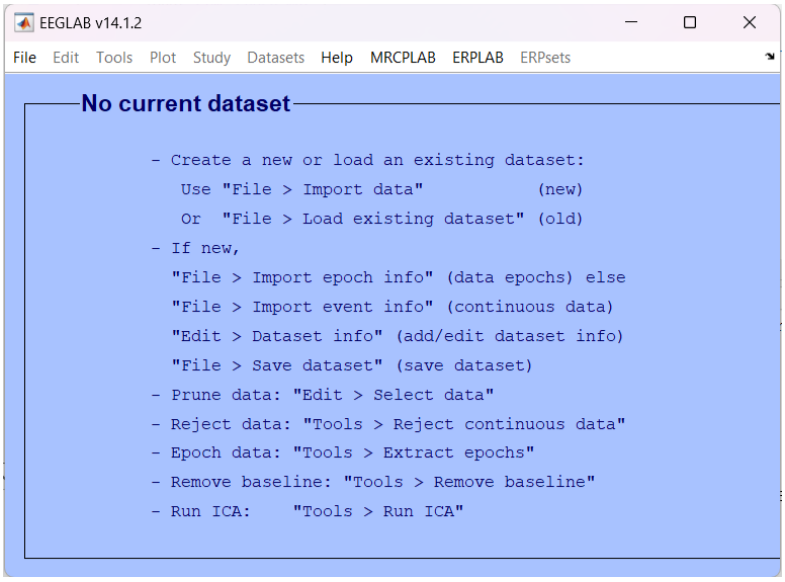

Figure 4.3: EEGLAB interface.

4.3.2 MRCPLAB

MRCPLAB is an EEGLAB plug-in developed specifically for this project. It interacts and exploits some of the EEGLAB functions, but it also introduces new ones more specific. Running EEGLAB, it is possible to use MRCPLAB from its menu where the following functions are displayed:

- *Import/Save data* is used to import datasets in two ways:
  - *Import from ASCII file*, it processes ASCII file data resampling and filtering EEG, EMG and EOG signals, evaluating the events, initializing the EEG structure with all the data needed and creating a .set file useful for faster successive uploading;
  - *Import from .set file*, it imports the EEG structure previously imported and processed from the ASCII file.
- *EEG Channel operation*, it contains all the function useful to process the continuous EEG signal:
  - *Channel data (scroll)* opens a window where it is possible to visualize the EEG and the onsets obtained from the EMG;
  - *Seek noisy channels* permits to evaluate bad channels which has to be rejected in order to obtain accurate results;
  - *Select or reject data* allows the rejection of bad channels;

  - *Artifact Correction* detects and corrects artifacts through ICA;
  - *Interpolate electrodes* interpolates previously rejected channels considering the closest electrodes;

- *Spatial Filter*, it allows to apply different type of spatial filters (SISF,SLSF,LLSF) with a variable number of electrodes and coefficients (all equal or SNR dependent); it is important to notice that SNR dependent coefficients can be used only if SNR has been estimated previously, otherwise, spatial filtering can be applied only with all equal coefficients;

- *Epoch operation*, it contains operations applicable on epochs:

  - *Epoch and filter* creates epochs according to the onsets evaluated through the EMG;
  - *Jitter compensation* allows to apply different methods for delay correction:
    - *RIDE* aligning the epochs applying residue iteration decomposition;
    - *Jitter compensation*, which aligns all epochs according to a channel selected by the user (Woody's method);
    - *Jitter compensation 1*, which aligns all epochs to a mean delay calculated over the seven channels of interests (Woody's method);
    - *Jitter compensation 2*, which performs alignment for different brain zones (Woody's method).
  - *ERP and SNR evaluation* calculates the ERP and corresponding SNR through averaging;
  - *ERP viewer* plots the ERP and SNR.

- *Topographies and Energy considerations* plots the topographies and prints energy consideration useful for LRP calculation.

Chapter 5

Artifacts

In this chapter, it is presented the definition of artifact and the description some types commonly found in EEG signals.

5.1 Definition of artifact

The electric signals recorded by EEG is attenuated due to the presence of tissue, bone and hair, but also other sources can introduce noise. The term artifact in EEG denotes any kind of signal not directly produced by human brain activity and can be physiologic, electric or environmental. Physiologic artifacts are produced by the body itself: eye movement, blinking, muscle contractions, heart beating, sweating, head movements. Electric and environmental artifacts are generated by outside sources mainly due to electrodes failures, cable movements or electromagnetic interferences.[20][32][33]
Artifacts bring three problems to the RP calculation:

- the decrease of Signal-to-Noise Ratio (SNR) and, therefore, the decrease of differentiation between conditions;
- the unlikelihood elimination of some artifacts by the averaging process due to their systematic property especially in some conditions;
- the change of sensory input caused by ocular artifacts[20].

The main artifacts that can be present in an EEG recording are: ocular, muscular, cardiac, sweat and electrode artifacts.

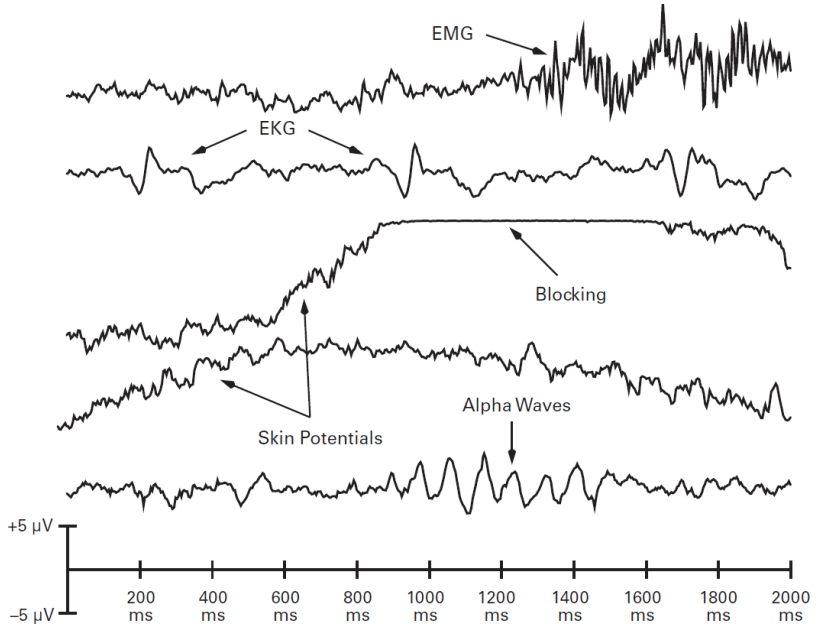

Figure 5.1: Some of the artifacts which can affect the EEG signal. Taken from [20]

5.1.1 Ocular artifact

Eye can be electrically modelled as magnetic dipole with positive charge in the cornea and negative in the retina. Therefore, blinking or moving generates a distortion of the electric field in the interested region. Generally, ocular movements can be recorded by Electrooculogram (EOG), vertical for blinking or vertical movements, or horizontal for lateral eyes movements.

Blinking. When the eyes blink, they slightly roll up (Bell's phenomenon) and the eyelid moves across the eyes acting as a variable resistor changing the voltage near the eyes. The monophasic deflection produced is 50 µV–100 µV for 200 ms–400 ms. The electrodes more affected by this artifact are the frontal ones, in particular Fp1 and Fp2, but also Fpz. They can be mistaken for frontal spike, but the characteristic of the opposite polarity above and below the eyes can be useful to identify the artifact and also remove it.

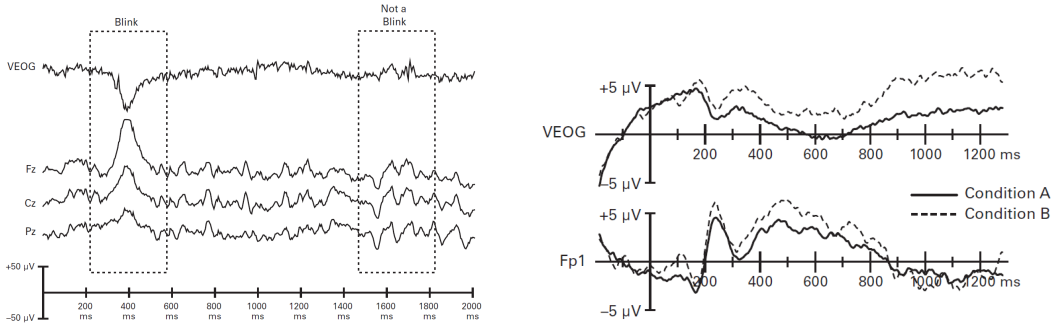

(a) **(b)**

Figure 5.2: Effects of blinking on different channels. Taken from [20]

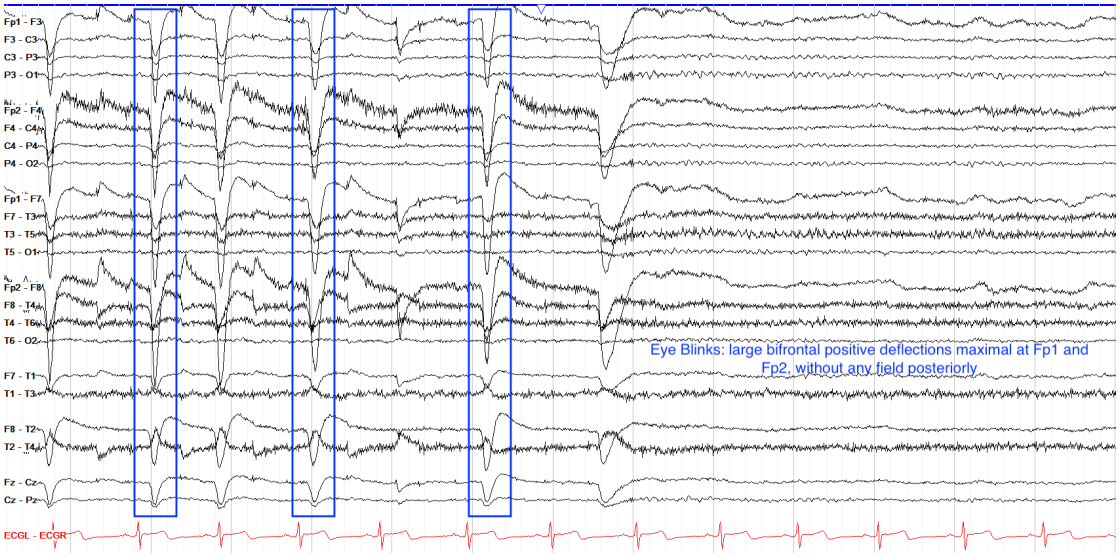

Figure 5.3: EEG affected by blinks. Taken from [33]

Lateral movement. As long as the eye's position does not change, the EEG will register a static voltage gradient easily removed with a baseline correction. Instead, when the eyes moves, the electrical potential of frontal electrodes will have different behaviour for each side of the head. For example, moving horizontally to the left causes positive potential on the left side electrodes and negative on the right side. The majority of recorded eye movements usually are *saccades*, fast shifts in eye position, consisting in sudden step from a voltage level to another where it would remain until the eyes move back to previous position.[20]

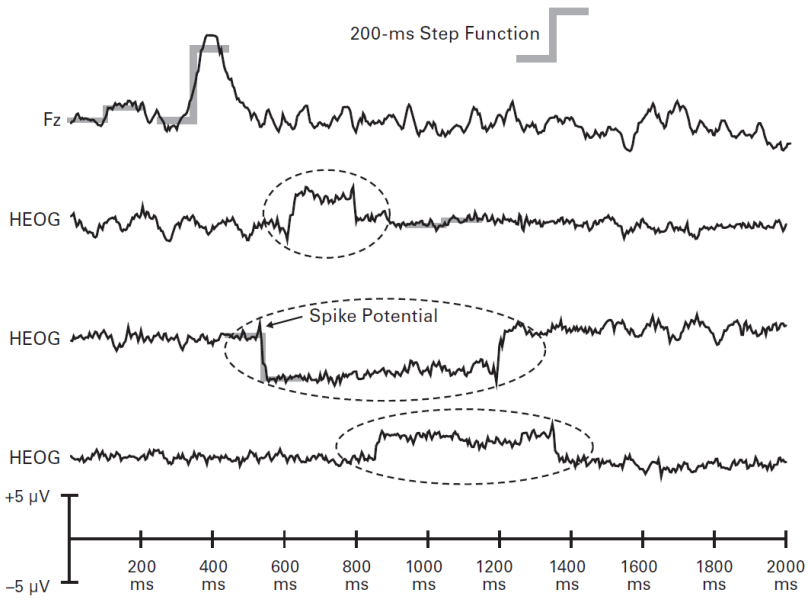

Figure 5.4: Effects of eye movements on EOG and Fz channels. Taken from [20]

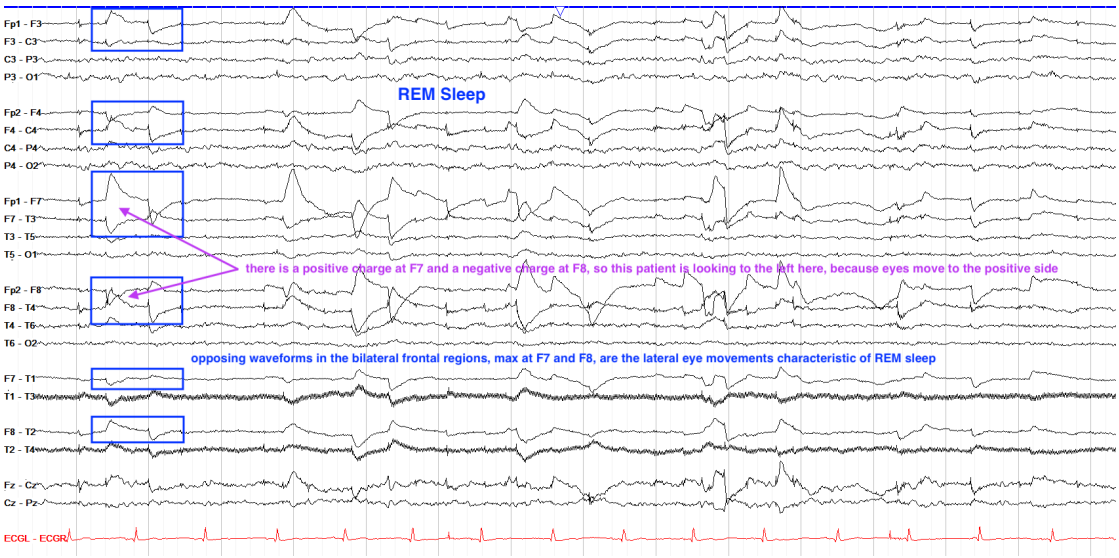

Figure 5.5: EEG during REM sleep characterized by the lateral movement of the eyes. Taken from [33]

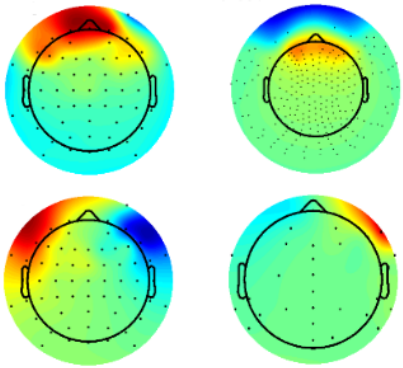

Figure 5.6: Topographies of the ocular artifacts. Taken from [34]

5.1.2 Muscular artifact

Muscle contraction produces measurable rapid voltage fluctuations that can interfere with EEG activity: chewing or the jaws' contraction can affect temporal electrodes; forehead's muscles can add high-frequency noise to Fp1 and Fp2; inferior occipital and temporal electrode sites can be affected by muscles of the neck. The high amplitude and frequency is usually visible and can be removed with a low-pass filter with a cut-off frequency between 30 Hz and 100 Hz. However, it is always better to have subjects relaxing the relevant muscles to minimise artifacts. Reflexive muscle twitches are quite problematic because they are sudden, high-frequency voltage changes limited to a very short time period and, therefore, very difficult to detect. [20][33]

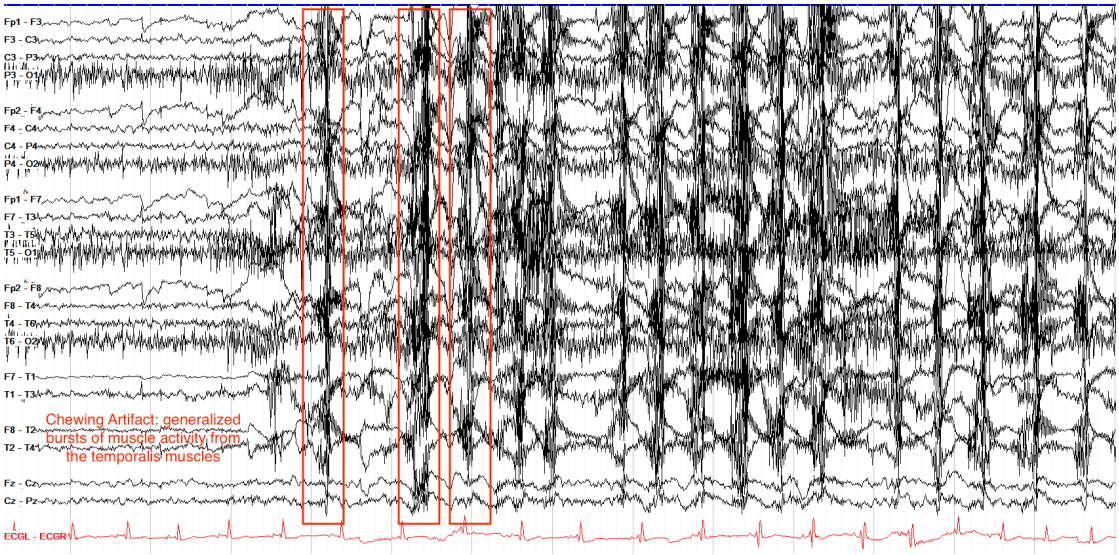

Figure 5.7: EEG affected by chewing. Taken from [33]

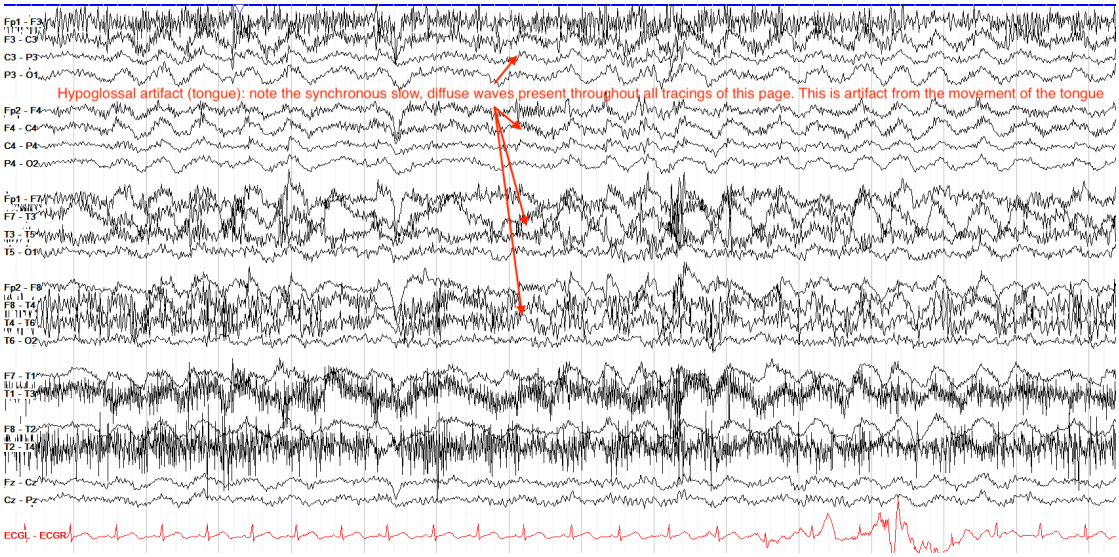

Figure 5.8: Hypoglossal artifact. Taken from [33]

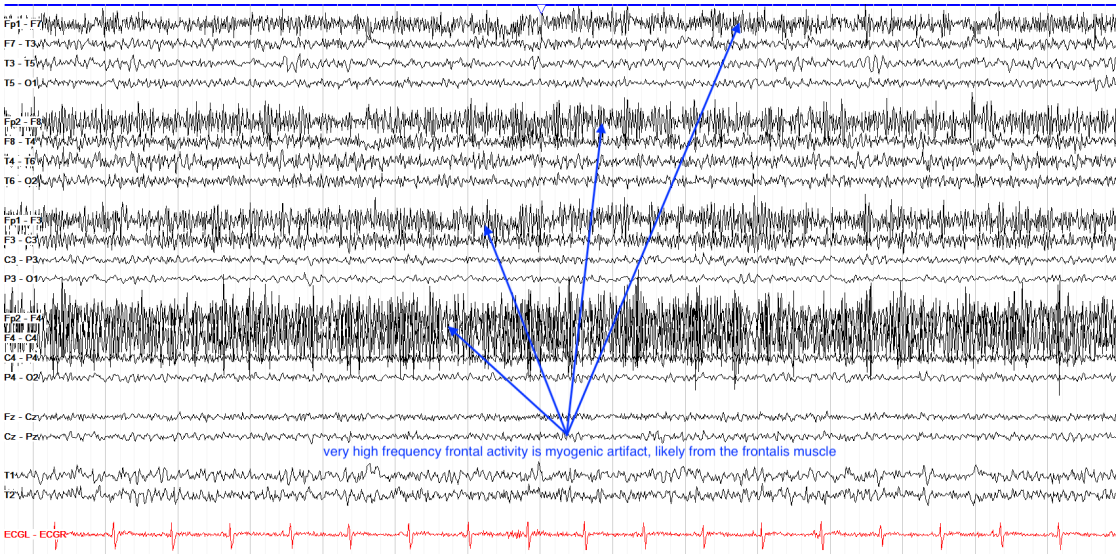

Figure 5.9: EEG during muscle contraction. Taken from [33]

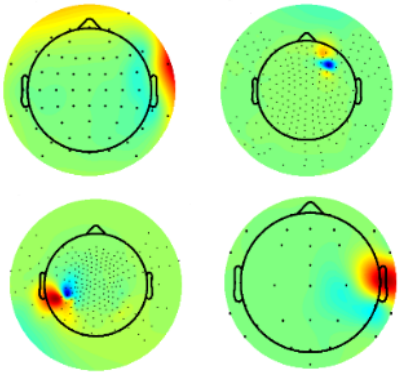

Figure 5.10: Topographies of the muscular artifacts. Taken from [34]

5.1.3 Cardiac artifact

In some EEG recordings it is possible to observe the beating of the heart. It is propagated through the carotid arteries and can be recorded by mastoid electrodes. To avoid this artifact, it is possible to slightly move the position of mastoid electrode, but nothing more than that. However, it is not systematic and it will just reduce the overall SNR. It can be useful to record the electrocardiogram (ECG) and use it to detect and remove the artifacts.[20][33]

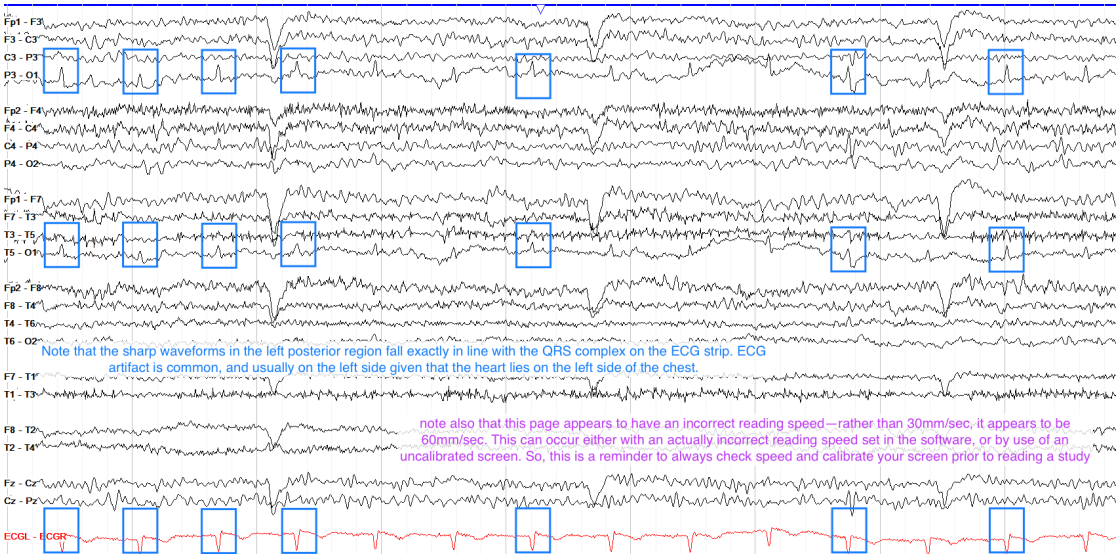

Figure 5.11: Cardiac artefact affecting the EEG. Taken from [33]

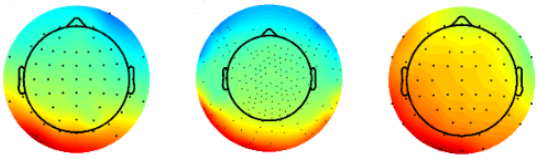

Figure 5.12: Topographies of the cardiac artifacts. Taken from [34]

5.1.4 Sweat artifact

When sweat begins to accumulate in glands, the skin impedance changes and potentials arise for many seconds. The same artifacts can be caused by slow shifts of electrodes if the subject moves. The waves overlapping the EEG signal have frequency less than 0.5 Hz and do not follow a particular localization, it is possible to correct them with a high-pass filter.[33]

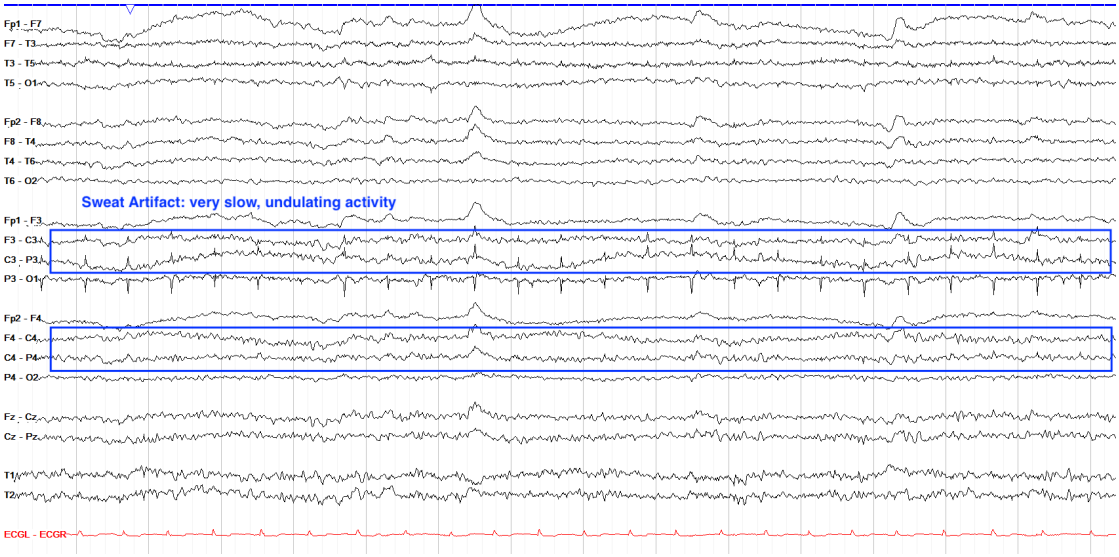

Figure 5.13: Slow waves due to sweating in EEG. Taken from [33]

5.1.5 Electrode artifact

Electrodes can give artifact caused by interference from the electrical activity or by becoming loose. In the first case, the effect can be a high amplitude interference on a single channel and it is possible to use a notch filter to remove it; while electrode pop is sudden and distort the signal in a very unpredicted way.[33]

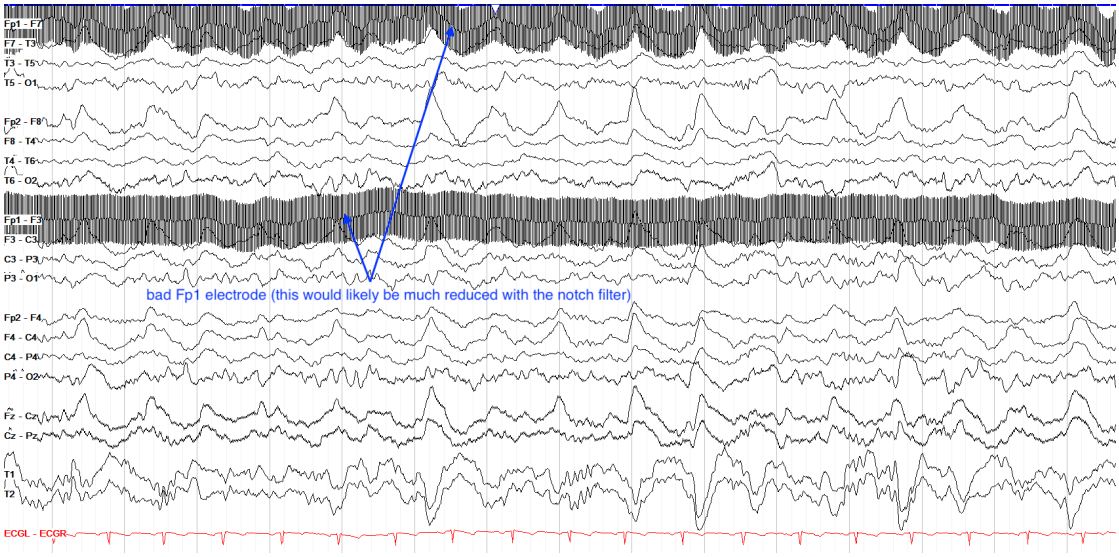

Figure 5.14: Electrode artifact due to interference from the electrical activity.

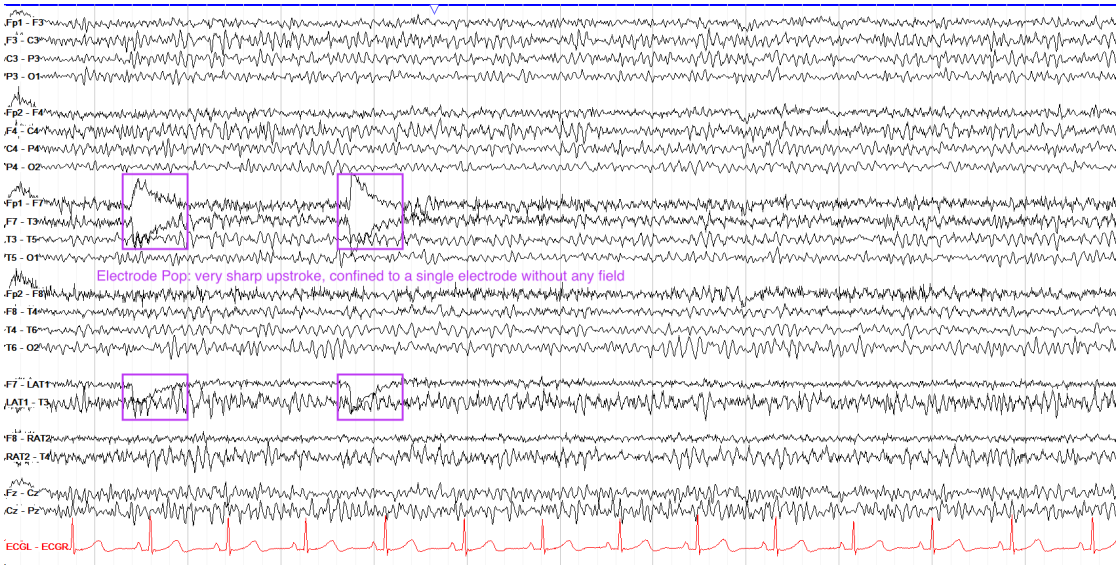

Figure 5.15: Electrode pop artifact. Taken from [33]

Chapter 6

Artifact detection and correction

The presence of artifacts can affect EEG signals and RP calculation misleading the classification. It is important to distinguish artifacts from brain waves, but it can be difficult because artifacts can be disorganized, intermixed with non-artifactual signal or look similar to cerebral signals. Therefore, the first problem to face is the detection of artifacts in EEG recordings. The second step is the minimization of artifacts' effects which can follow two ways: artifact rejection, which excludes trials containing clear artifacts, or artifact correction, estimating the influence of artifacts and then subtracting it. The former works well, but brings the risk of throwing out a number of trials which reduce the statistical power of the averaged ERP; on the other hand, the latter can exploit different procedures, but they may not work well in all situations, generate distortions or not consider fast input changes. Despite the cited drawbacks, one of the most popular and efficient method for artifact detection and correction is Independent Component Analysis (ICA) which exploits statistical properties to extract a set of components and isolate artifacts. The automated algorithm implemented in MRCPLAB uses ICA and performs a detailed analysis on components and applies correction.
In this chapter, it will be introduced the ICA, the analysis components in frequency and time domain for detection, the enhancements applied to the algorithm and the results obtained.

6.1 Independent Component Analysis

Before explaining how Independent Component Analysis works, it is better to take a step back and remind how sources in brain mix. As previously explained, the pyramid cells generate postsynaptic potentials whose summation allows the

recording at the scalp.
The minimum conditions to have a measurable signal on the scalp are:

- the concurrent activation of a large number of neurons;
- the approximately same orientation of individual neurons;
- the increase of postsynaptic potentials from the same part for the majority of the neurons;
- the same direction of current flow for the majority of neurons to avoid cancellation.[35]

The current flows through volume conduction, i.e. brain tissues, from neurons to the scalp. This causes spreading and voltage's distribution gets wider with the skull's high resistance. Therefore, the waveform recorded from any electrode on the scalp is a weighted sum of waveforms from different internal generators. The weights are determined by the position and orientation of each source with respect to the electrode site and the conductivity of brain tissues.[20]
The main interest is the estimation of individual sources from scalp recordings which represents a *forward problem* without a single solution. Different mathematical procedures were proposed and one of the most used today is Independent Component Analysis.

ICA is a special case of Blind Source Separation (BSS), i.e. the unmixing process not knowing any of the qualities of individual source signals. In particular, ICA exploits temporal independence to separate the signals.
The most intuitive example to better understand ICA application is the "cocktail party problem": when we are at a party in a crowded room with music and a lot of people talking, but we are interested in hearing what a single person, far from us, is saying. Recording with microphones positioned in different places, ICA is able to separate all the voices and sounds in the room and to focus the attention on one voice or sound.
Considering the signal recorded at the scalp X, ICA looks for the unmixing matrix W to decompose the signal into Independent Component signals U, also called IC activations. Algebraically,

$$U = WX \tag{6.1}$$

The inverse of the unmixing matrix, W^{-1}, is the mixing matrix which recaptures the scalp data through multiplication with the IC activation matrix ($X = W^{-1}U$), as shown in 6.1. This source separation process is suited for

1. independent sources;

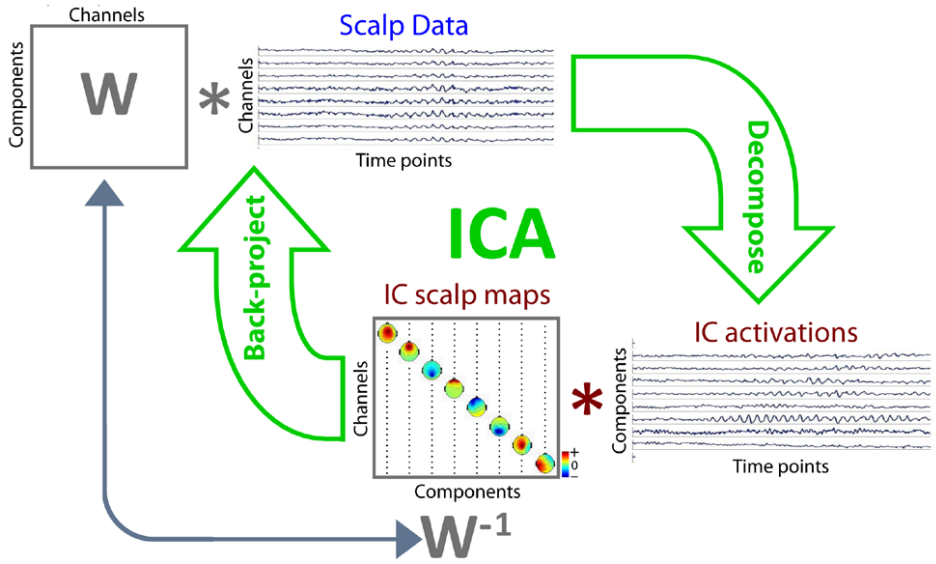

Figure 6.1: Schematic flowchart of ICA process of decomposition and back-projection. Taken from [35]

2. negligible propagation delay of the mixing medium;
3. analog sources with probability distribution not precisely Gaussian;
4. the number IC components equal to the number of sensors.

For EEG signals, the first two assumptions can be considered as satisfied: the EEG dynamics can be modelled as a collection of statistically independent brain process (1) and the volume conduction is instantaneous (2). The third assumption is plausible for EEG sources usually sparsely active and then far from normal distribution. The fourth assumption is questionable since it is not known the effective number of statistically independent sources of EEG recordings. Then, it is suggested to use an adequate amount of data to recognize independence and obtain a successful ICA decomposition.[20][35]

6.2 Automated Algorithm

This thesis focuses on the enhancements of the automated algorithm dedicated to artifact correction.
The process is composed by three fundamental steps:

1. evaluation of Independent Components;

2. detection of artifactual components;

3. correction and reconstruction of the signal.

6.2.1 Evaluation of Independent Components

The matrix of recorded signals is imported to evaluate the Independent Components through the function *runica.m* provided by EEGLAB. This function exploits the algorithm developed by Bell and Sejnowski (1995). They studied a self-organising learning algorithm which maximises the transferred information in a network of non-linear units without assuming any prior knowledge of input distributions. The non-linearities in the transfer function allow to find higher-order moments of the input distributions and perform redundancy reduction between output units. In other words, the neural network looks for the weights maximizing the joint entropy and minimizing the mutual information.[36] In particular, the minimization of mutual information is possible through the natural gradient studied by Amari, Cichocki and Yang. Given the weights, their multiplication with the recorded data separates statistically independent components. Therefore, given a signal matrix $n_{Ch} \times t$, where n_{Ch} is the number of channels and t the time expressed in samples, from the *runica* function is obtained the activation matrix $n_{IC} \times t$, the weights matrix $n_{IC} \times n_{Ch}$ and the sphere matrix $n_{Ch} \times n_{Ch}$ (i.e. matrix removing correlation between components).

$$activation = weights \cdot sphere \cdot EEGdata \tag{6.2}$$

When EOG signals are available, they are added to the data matrix before ICA in order to improve the ocular artifacts' detection.

Once the activation components are obtained, it is possible to proceed to the next step.

6.2.2 Detection of Artifactual Components

The algorithm aims at detecting ocular and muscular artifacts, and focal components typical of noisy channels. The integration of EOG signals, when available, makes possible the detection of ocular artifacts through the Pearson's correlation coefficient. It gives a measure of the linear dependence between two variables A and B as

$$\rho(A, B) = \frac{cov(A, B)}{\sigma_A \sigma_B} \tag{6.3}$$

where $cov(A, B)$ is the covariance of the two variables, σ_A and σ_B their standard deviation. The Matlab function *corrcoeff* evaluates ρ for each component and the left and right EOGs. The IC with maximum ρ is identified as artifactual and

corrected immediately. Successively, the algorithm evaluates specific features for each IC in frequency and time domain:

- **Fit-error:** it describes the deviation of a component's spectrum from a prototypical curve and its shape defined as $\frac{1}{f}$ where

$$f \mapsto \frac{k_1}{f^\lambda} - k_2 \tag{6.4}$$

  The parameters k_1, λ and k_2 are strictly positive and they are determined by three points in the log spectrum: value at 2 Hz, the local minimum in the band 5 Hz–13 Hz and the local minimum in the band 33 Hz–39 Hz.[37]

- **Average log band power:** the average logarithmic power is evaluated in two bands: 8 Hz to 13 Hz for non-artifactual components and 25 Hz to 40 Hz for muscular components. [37]

- **Focal components:** measure given by the maximum z-score of the mixing matrix W^{-1} [38]:

$$F = \max\left(Z(W^{-1})\right) \tag{6.5}$$

- **Kurtosis and Skewness:** they are statistical properties of data; kurtosis gives a measure of sharpness of a distribution's peak and it is evaluated as

$$K = \frac{E\{(x-\mu)^4\}}{\sigma^4} - 3 \tag{6.6}$$

  When a distribution has high kurtosis w.r.t. the normal distribution, it is called leptokurtic, otherwise it is said platykurtic. Skewness measures the symmetry of a probability distribution as follow

$$Sk = \frac{E\{(x-\mu)^3\}}{\sigma^3} \tag{6.7}$$

  They are used to analyse the signal and identify ocular and cardiac artifacts.

- **Entropy:** it can be interpreted as a statistical measure of randomness and it is evaluated as

$$H = -\sum p(x)\log_2(p(x)) \tag{6.8}$$

  where $p(x)$ is the probability of observing the activity values of x in the distribution. The more unpredictable, i.e. with low probability values, components have large entropies; on the other hand, high probability variables have small entropy.

The thresholds of fit-error and average log power have been evaluated statistically through an Expectation-Maximization algorithm. The threshold for focal components has been set to 1.5. Kurtosis, skewness and entropy have been normalized by trimmed mean which normalizes a variable without considering the 0.1% of the lowest and highest values. For those features, the threshold is set to 5.
These settings permit the individuation of artifactual components:

- ocular artifacts are detected through correlation coefficient with EOG;
- muscular artifacts are characterized by low fit-error and peak in the 25 Hz–40 Hz band;
- eye blinking, cardiac and intense muscular artifacts presents leptokurtic distributions;
- noisy channels show high focal components;
- other unpredictable and unexpected artifacts will be characterized by high entropy.

6.2.3 Correction and Reconstruction of the Signal

The final step after detection is correction of artefactual components by setting them to 0. In this way, during the reconstruction of the EEG signal multiplying the IC by the mixing matrix, the components considered artifacts will have a minimum weight and will not influence the final result.

6.3 Results

The Artifact Correction algorithm is applied after rejecting bad channels to avoid their influence in the analysis and detection. After correction, the bad channels are interpolated with the closest ones. At this point, it is possible to apply spatial filtering or to epoch the data. Spatial filters are powerful tools to identify the lateralization of the RP (high-pass) or to increase the quality of the RP by removing noise (low-pass). Since the goal of this thesis is to prove the validity of the automated artifact correction algorithm, spatial filters are not applied and the continuous data are divided into epochs of 8 s identified by the EMG. The epoched data undergo to an algorithm compensating the jitter between different epochs and then are averaged to obtain the final RP and SNR. The SNR is obtained considering the noise as the difference between even and odd epochs, and it is an important feature in the machine learning algorithm.
In the following section, the results obtained with the original and enhanced version

of the algorithm will be presented.
The datasets are chosen between voluntary, involuntary and semi-voluntary tasks of the 2018 protocol, since the number of electrodes used is large enough to guarantee a good ICA. For each datasets, the figures shown are: the topographies of all ICs, giving an idea of the artifacts' influence on components; the ICs more correlated with EOGs; the kurtosis, skewness and entropy of each IC; the RPs and the corresponding SNR of the most relevant channels (Fc3,Fcz,Fc4,C3,Cz,C4,Pz) and lines (Pre-motor,Motor,Left hemisphere,Right hemisphere, Median Rostro-Caudal). Moreover, a table compares the components detected by each algorithm.
Note that the enhanced algorithm corrects first the IC detected with EOG and then compute all the other features; therefore, the entropies of those components are the highest, but they will not be reported as detected by entropy in the table.

From these results, it is possible to observe that the enhanced algorithm detect the components cited previously with an increase of SNR values.

6.3.1 Voluntary

For voluntary tasks, the RP should show two clear peaks: one close to zero, indicating the presence of intention; the second after zero, corresponding to the motor activity. The SNR should be positive at least in the interval close to zero; if the SNR is not positive, nothing can be said about the information in that time period.

Dataset GF892070

Artifacts	Previous AC	Enhanced AC
Ocular/EOG	-	2,4
Muscular	7	24,33
Focal	6	34,35
Kurtosis and skewness	All	1,5
Entropy	All	1,3

Table 6.1: GF892070 Voluntary task: IC detected and corrected.

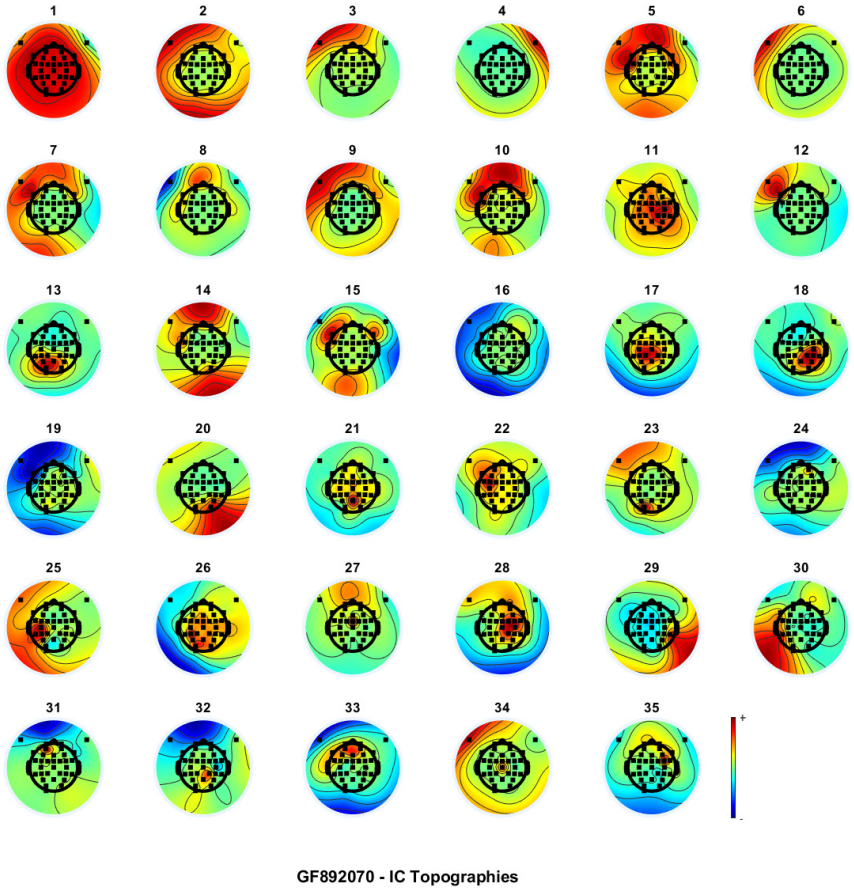

Figure 6.2: GF892070 Voluntary task: Topographies of IC.

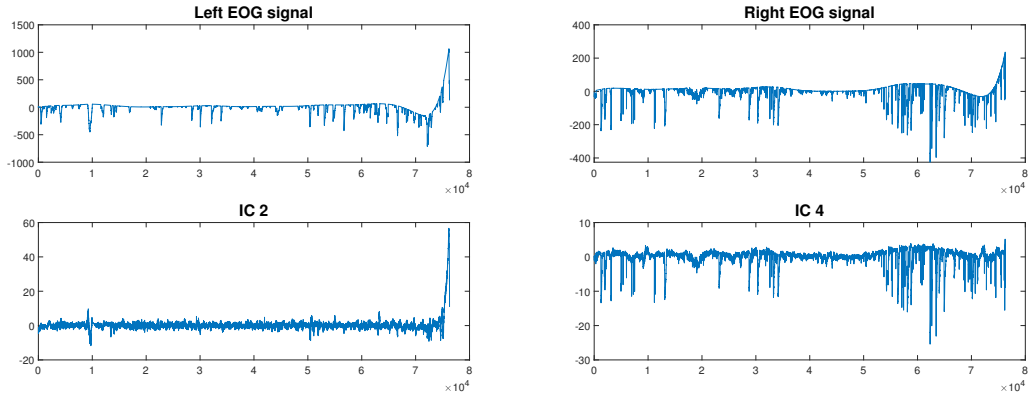

(a) **(b)**

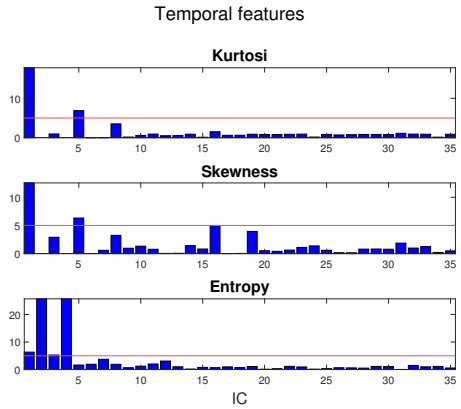

(c)

Figure 6.3: GF892070 Voluntary task: (a) and (b) show the EOG signals and the ICs more correlated with them; (c) reports the normalized value of kurtosis, skewness and entropy for each component and in red the threshold.

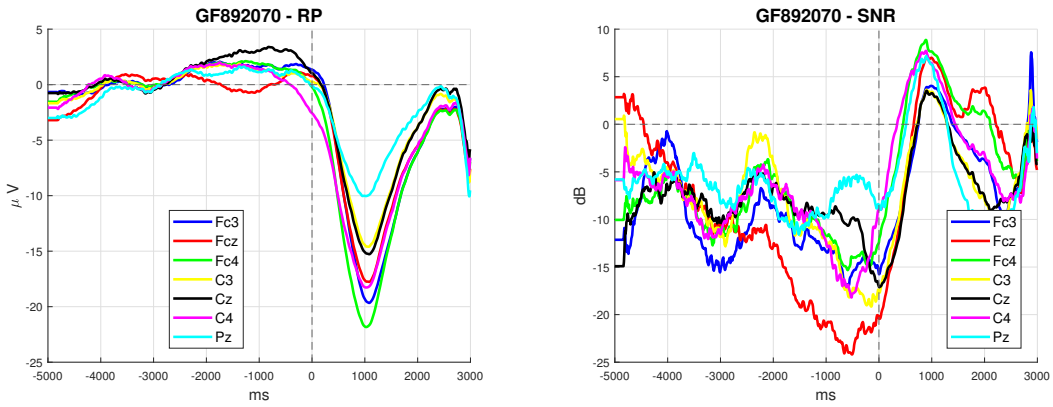

Old Artifact Correction algorithm.

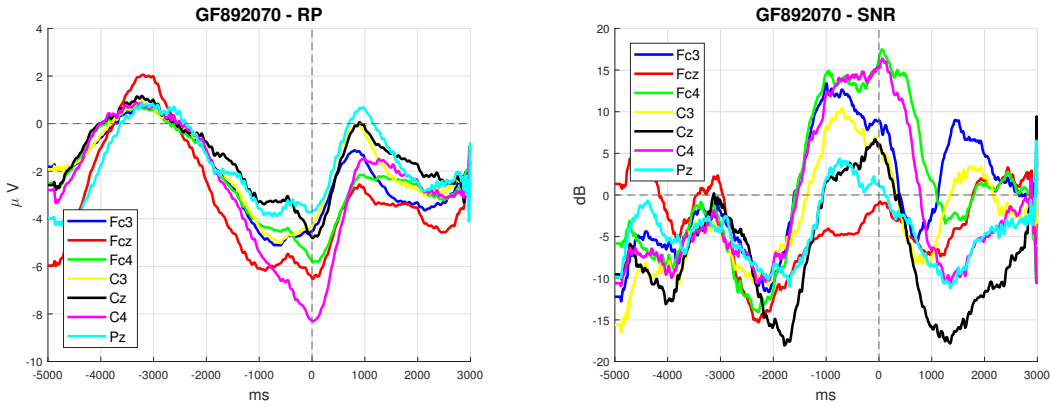

Enhanced Artifact Correction algorithm.

Figure 6.4: GF892070 Voluntary task: RP and SNR obtained with Woody's jitter compensation method.

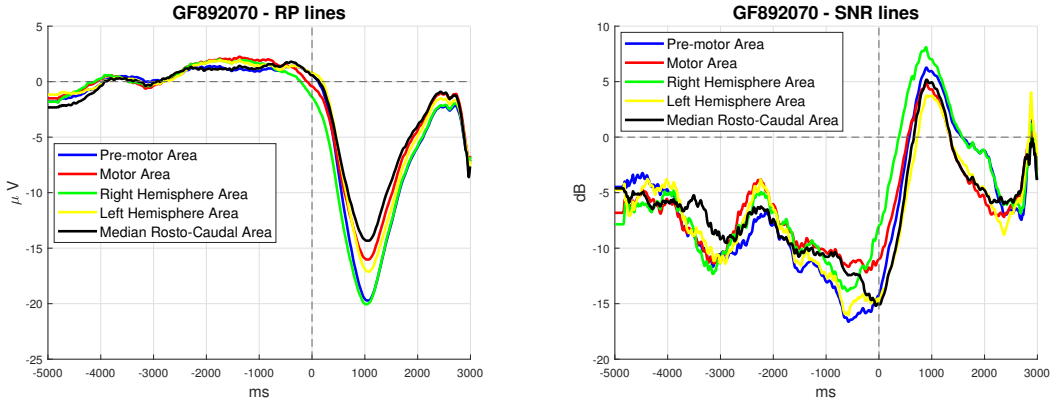

Old Artifact Correction algorithm.

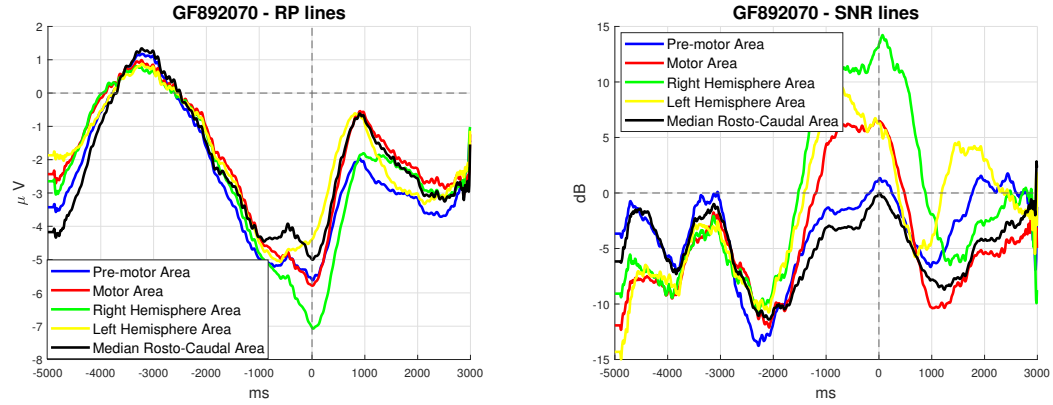

Enhanced Artifact Correction algorithm.

Figure 6.5: GF892070 Voluntary task: RP and SNR of averaged lines obtained with Woody's jitter compensation method.

Dataset AL858070

Artifacts	Previous AC	Enhanced AC
EOG	-	4,5
Muscular	-	2
Focal	2,8,10,16,29	34
Kurtosis and skewness	All	1,30,31,34
Entropy	All	-

Table 6.2: AL858070 Voluntary task: IC detected and corrected.

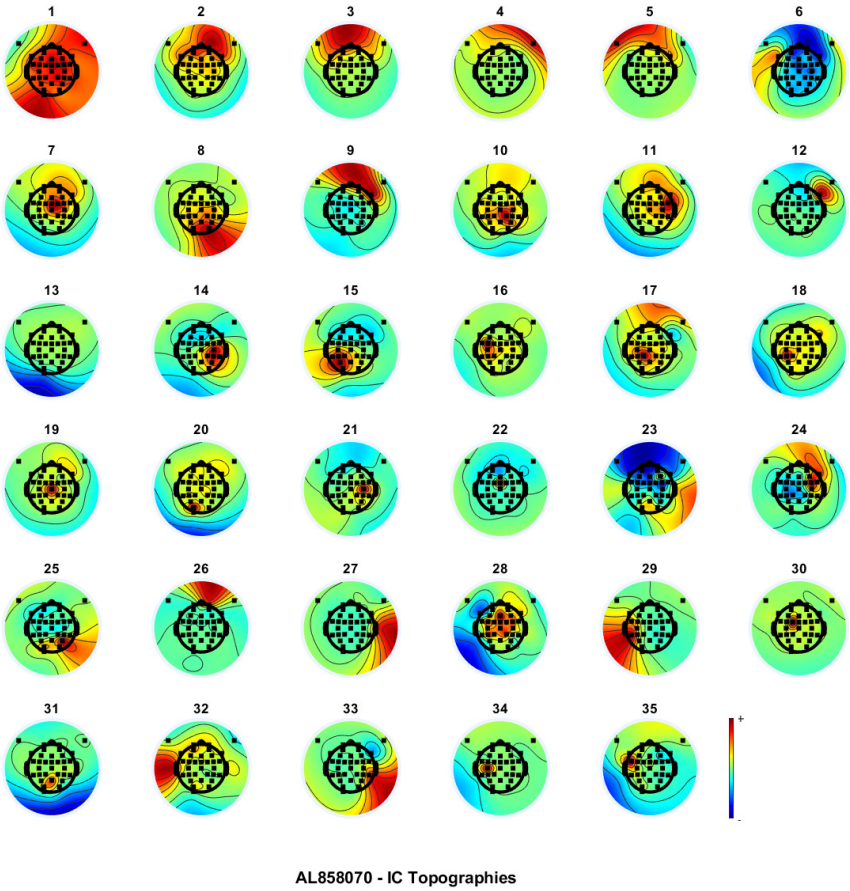

Figure 6.6: AL858070 Voluntary task: Topographies of IC.

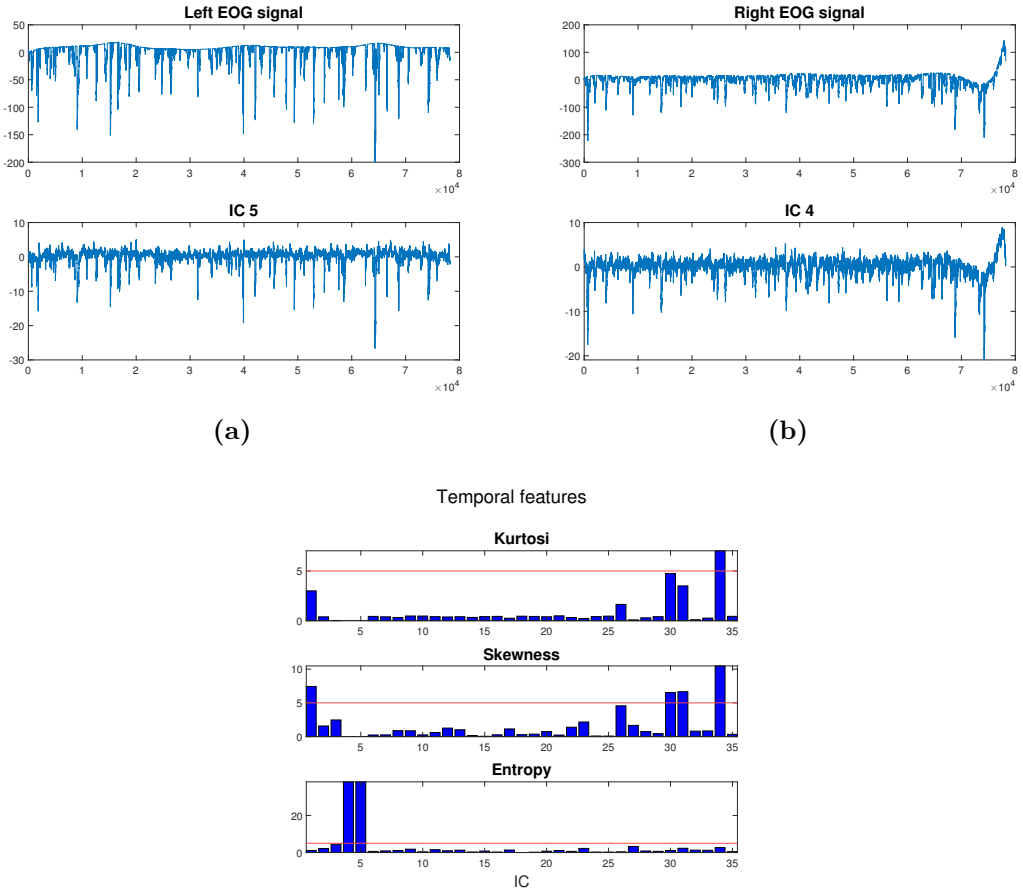

Figure 6.7: AL858070 Voluntary task: (a) and (b) show the EOG signals and the ICs more correlated with them; (c) reports the normalized value of kurtosis, skewness and entropy for each component and in red the threshold.

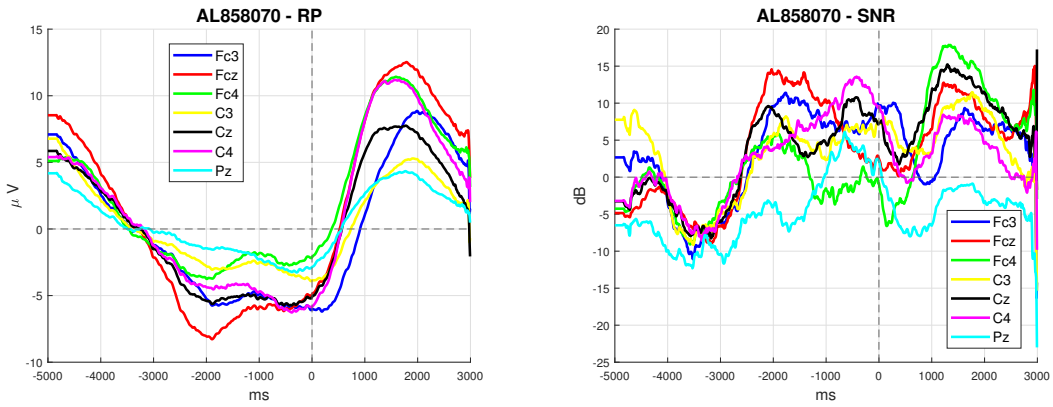

Old Artifact Correction algorithm.

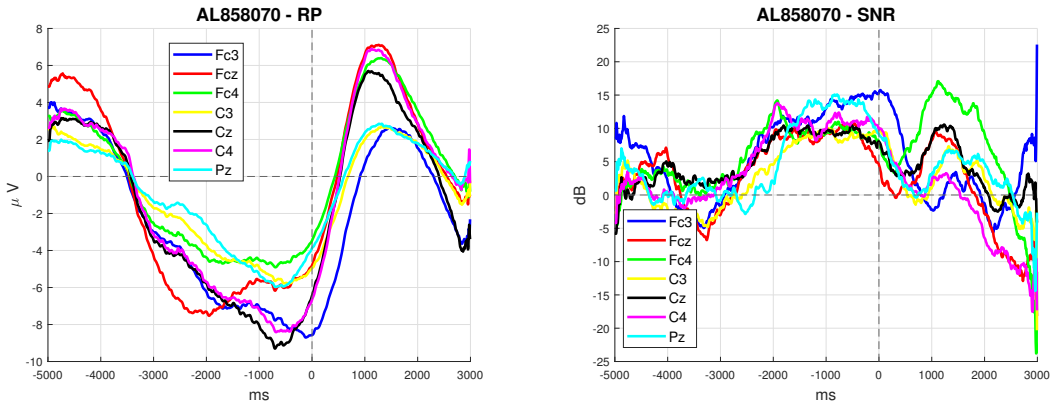

Enhanced Artifact Correction algorithm.

Figure 6.8: AL858070 Voluntary task: RP and SNR obtained with Woody's jitter compensation method.

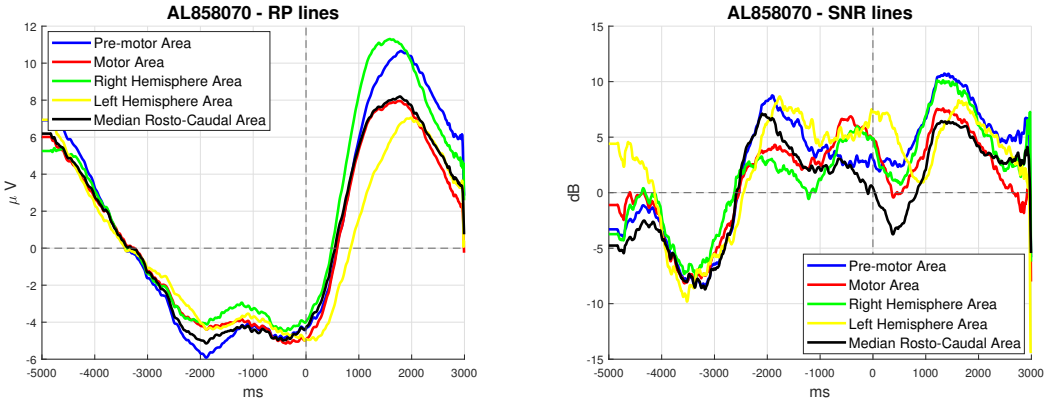

Old Artifact Correction algorithm.

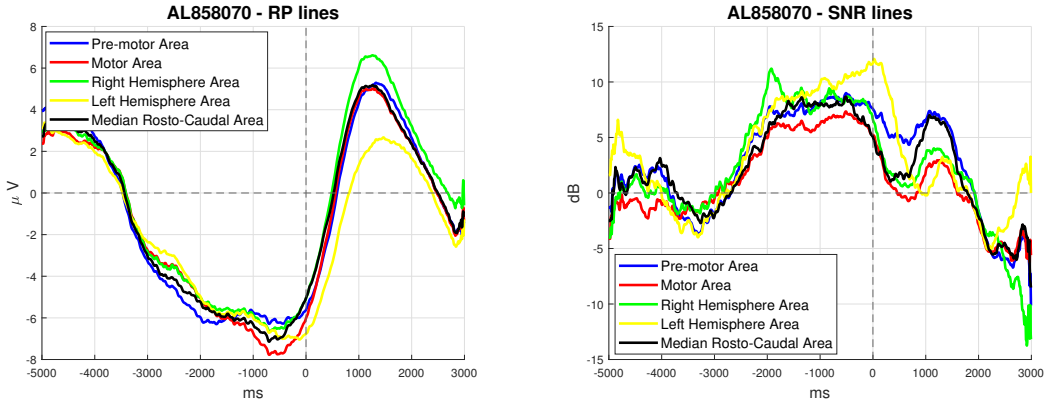

Enhanced Artifact Correction algorithm.

Figure 6.9: AL858070 Voluntary task: RP and SNR of averaged lines obtained with Woody's jitter compensation method.

Dataset MI993011

Artifacts	Previous AC	Enhanced AC
Ocular/EOG	1,8,21	1,5
Muscular	1,8,21	8,9,13,14,20,28,30,32
Focal	3,4,6,13	33
Kurtosis and skewness	All	2
Entropy	All	3,4

Table 6.3: MI993011 Voluntary task: IC detected.

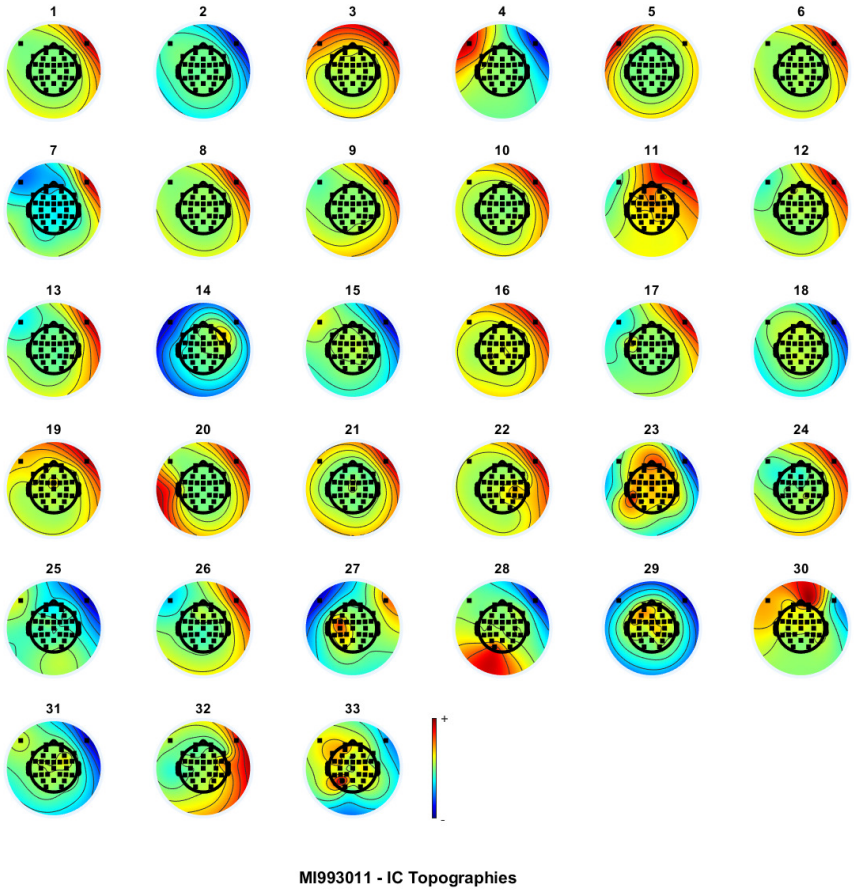

Figure 6.10: MI993011 Voluntary task: Topographies of IC.

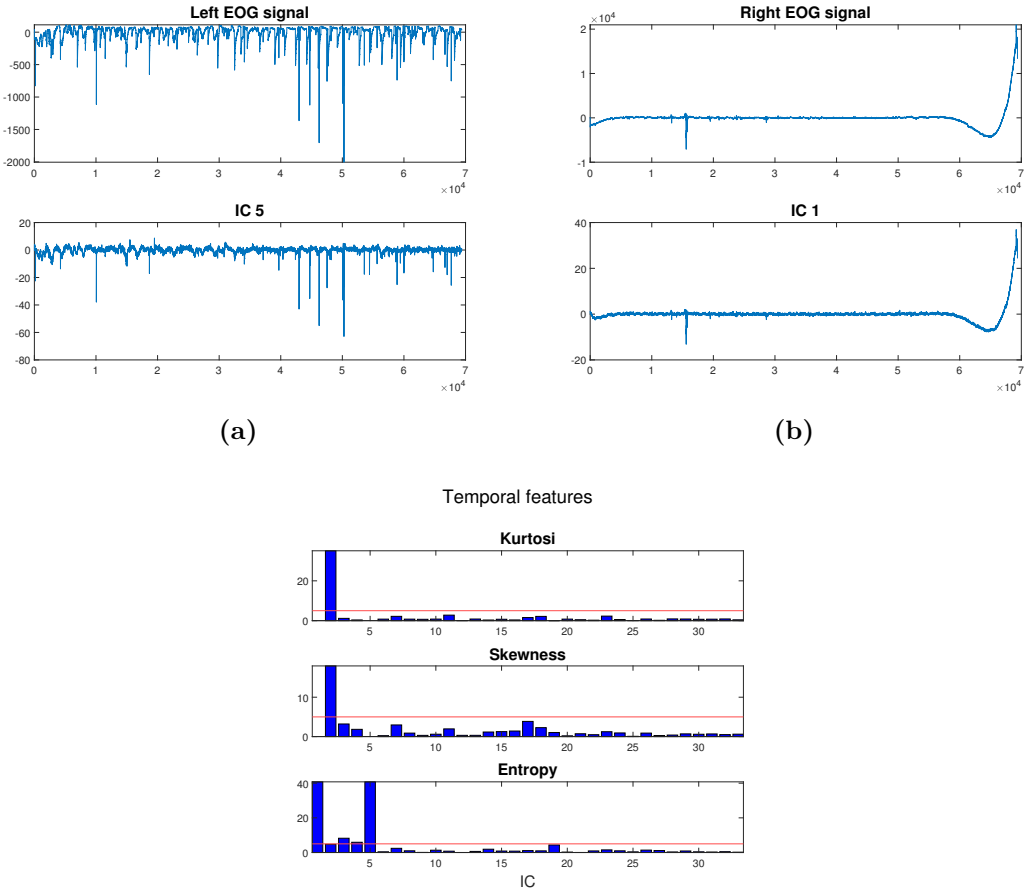

Figure 6.11: MI993011 Voluntary task: (a) and (b) show the EOG signals and the ICs more correlated with them; (c) reports the normalized value of kurtosis, skewness and entropy for each component and in red the threshold.

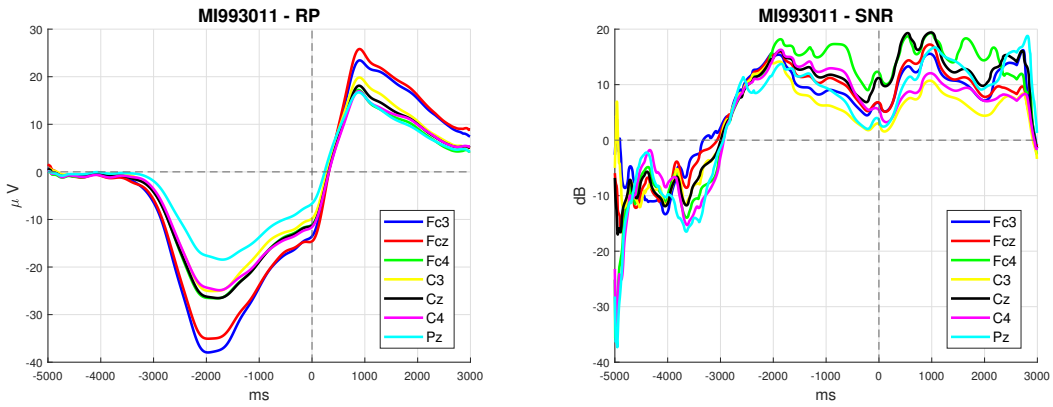

Old Artifact Correction algorithm.

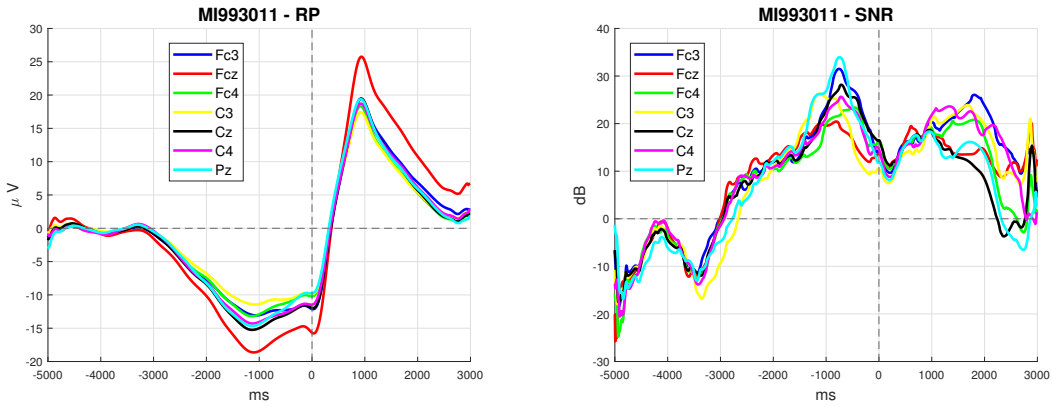

Enhanced Artifact Correction algorithm.

Figure 6.12: MI993011 Voluntary task: RP and SNR obtained with RIDE jitter compensation.

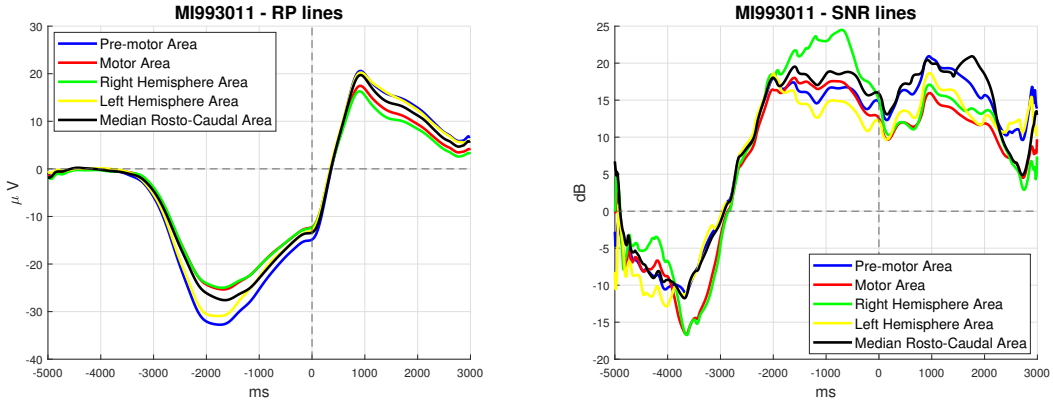

Old Artifact Correction algorithm.

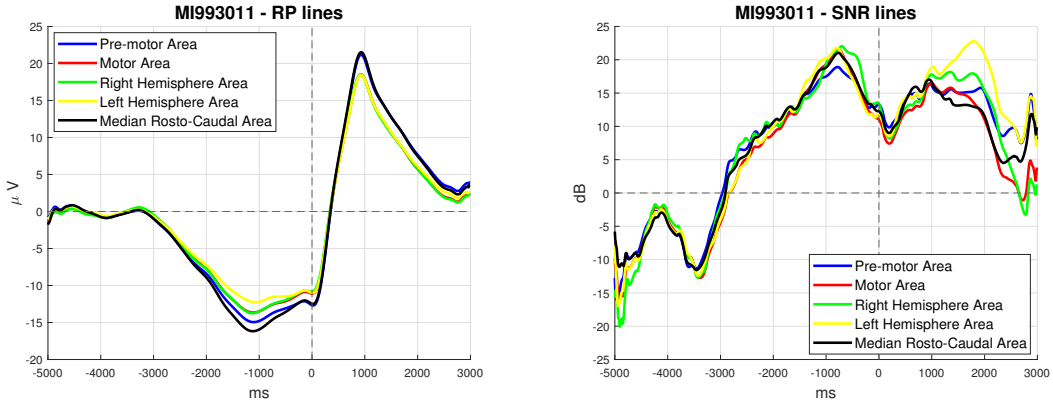

Enhanced Artifact Correction algorithm.

Figure 6.13: MI993011 Voluntary task: RP and SNR of averaged lines obtained with RIDE jitter compensation.

Dataset TC995011

Artifacts	Previous AC	Enhanced AC
Ocular/EOG	4,5,7,8,10,11,12,18,19,22,23,27	1,4
Muscular	10,12,27	8,9,12,13,15,16,30
Focal	3,6,13	32
Kurtosis and skewness	All	5,15
Entropy	All	2,5,7

Table 6.4: TC995011 Voluntary task: IC detected and corrected.

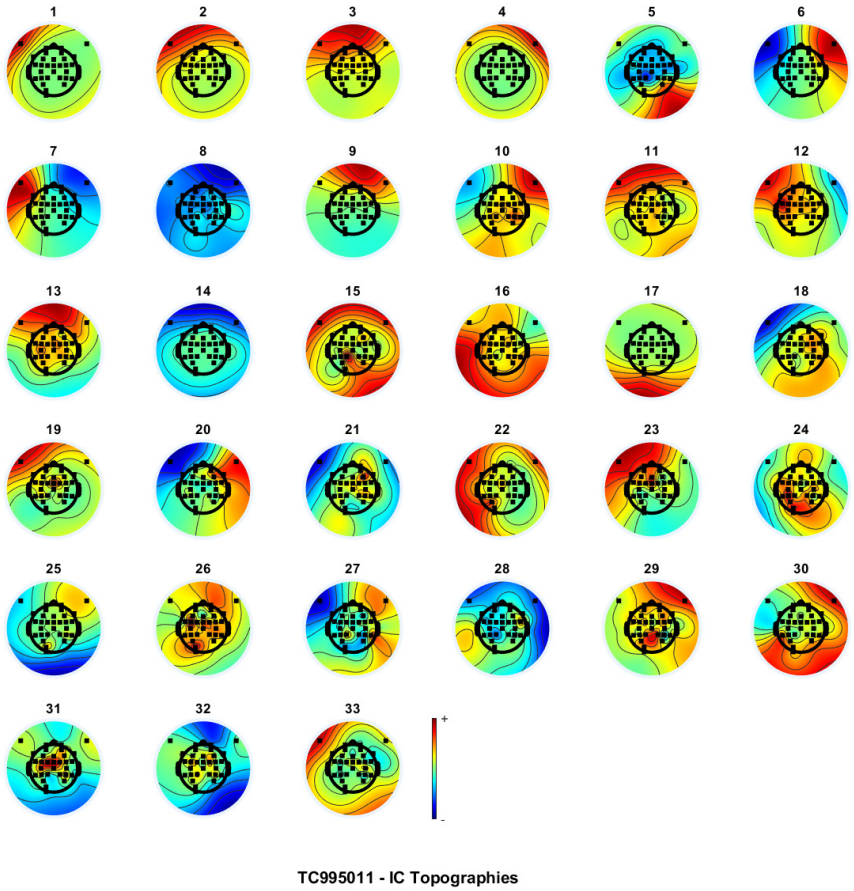

Figure 6.14: TC995011 Voluntary task: Topographies of IC.

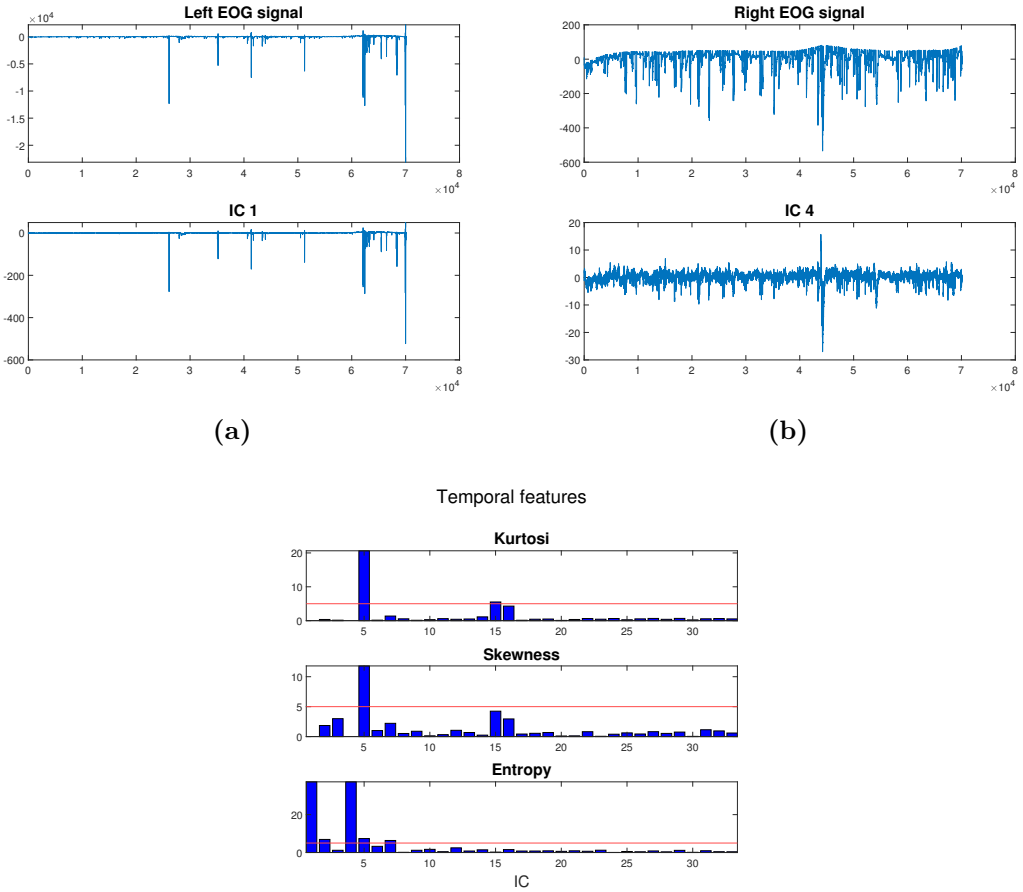

Figure 6.15: TC995011 Voluntary task: (a) and (b) show the EOG signals and the ICs more correlated with them; (c) reports the normalized value of kurtosis, skewness and entropy for each component and in red the threshold.

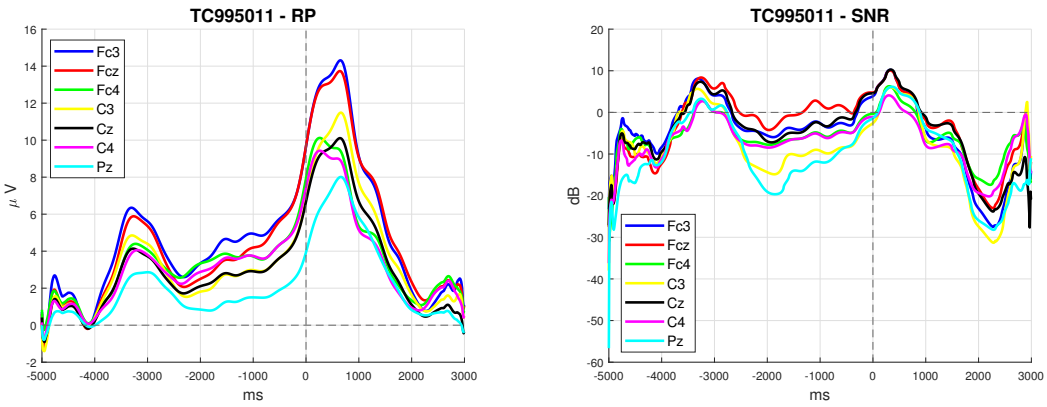

Old Artifact Correction algorithm.

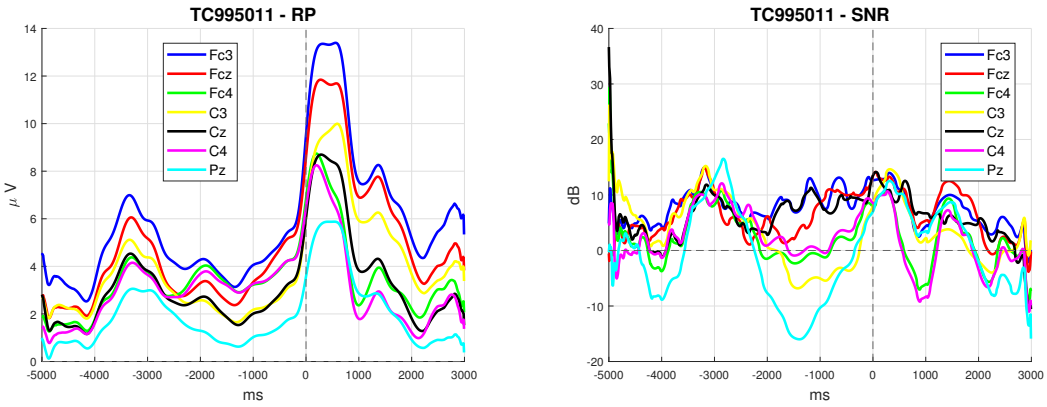

Enhanced Artifact Correction algorithm.

Figure 6.16: TC995011 Voluntary task: RP and SNR obtained with RIDE jitter compensation.

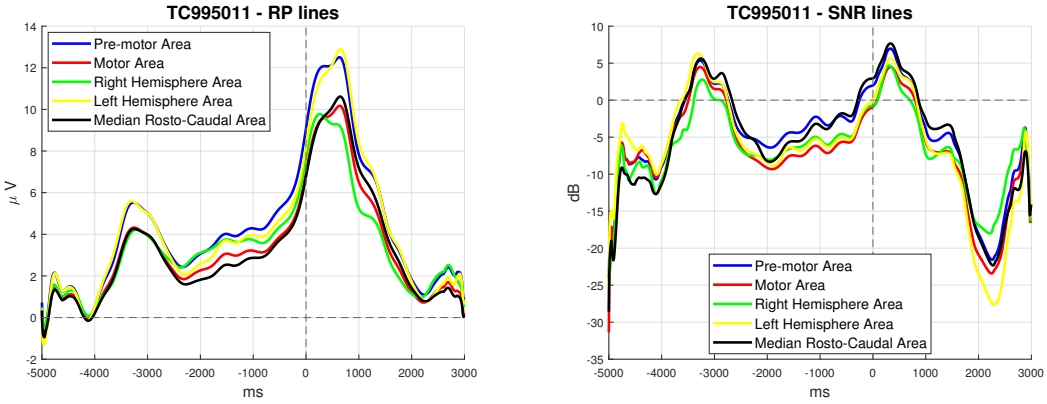

Old Artifact Correction algorithm.

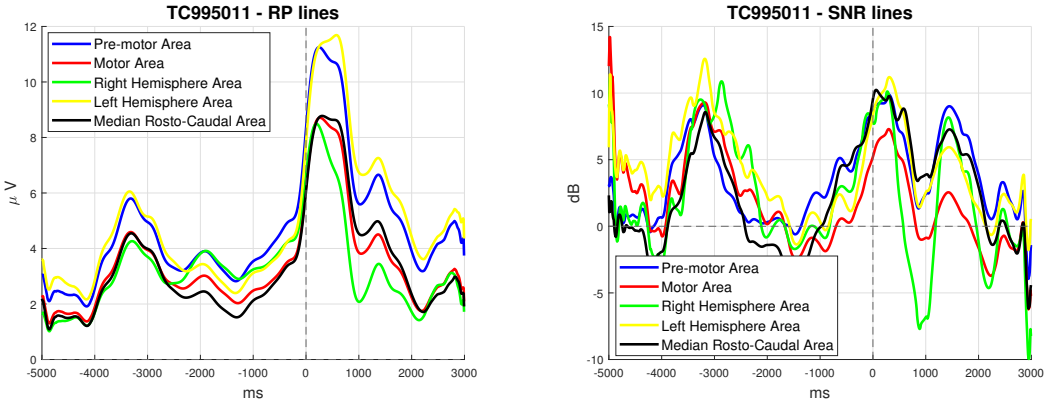

Enhanced Artifact Correction algorithm.

Figure 6.17: TC995011 Voluntary task: RP and SNR of averaged lines obtained with RIDE jitter compensation.

6.3.2 Semi-voluntary

The RP of a semi-voluntary task should present a lower peak of the intention due to the smaller preparation time of the subject.

Dataset AL858070

Artifacts	Previous AC	Enhanced AC
Ocular/EOG	1,2,6,21,22,32	1
Muscular	2,6,21,22,32	-
Focal	1 3 4	3,34,35
Kurtosis and skewness	All	5,8,12,14,35
Entropy	All	3,5

Table 6.5: AL858070 Semi-voluntary task: IC detected and corrected.

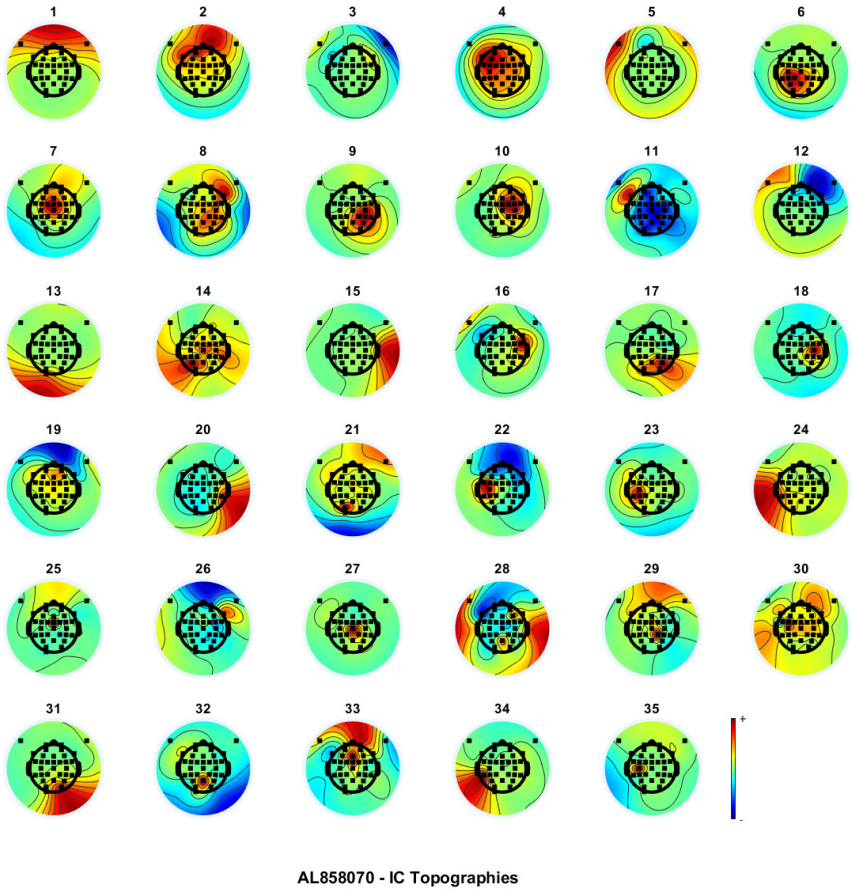

Figure 6.18: AL858070 Semi-voluntary task: Topographies of IC.

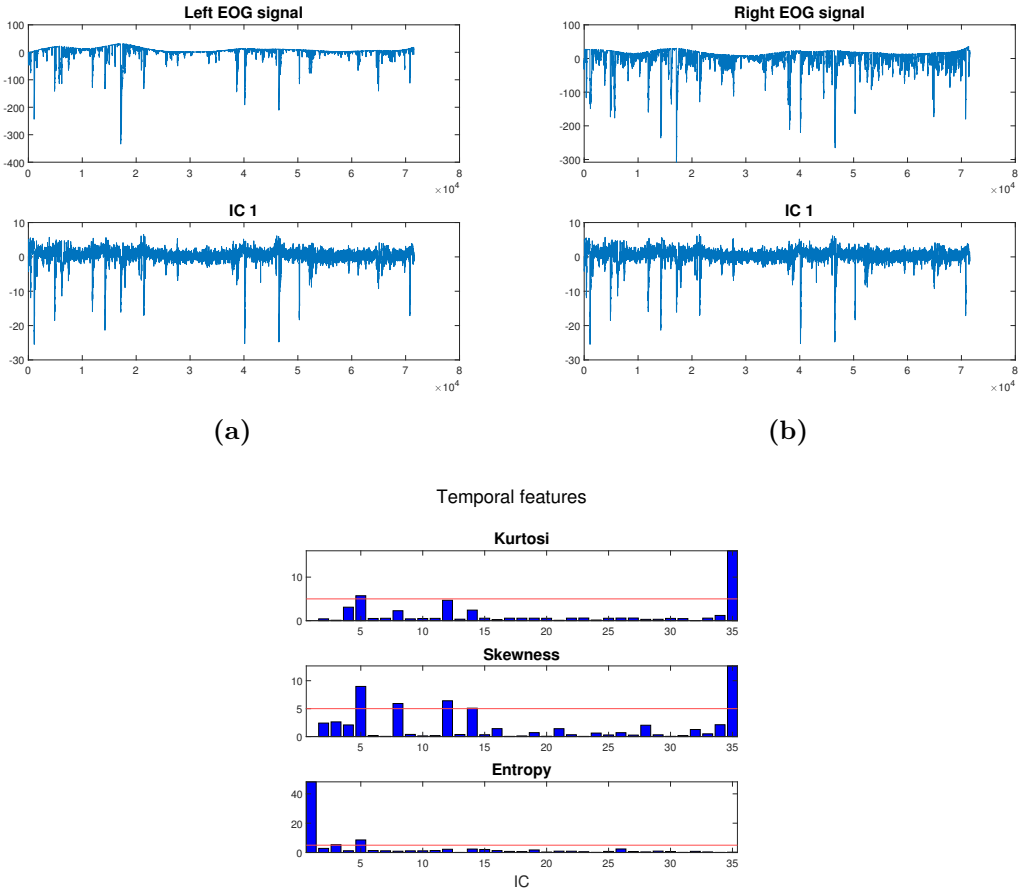

Figure 6.19: AL858070 Semi-voluntary task: (a) and (b) show the EOG signals and the ICs more correlated with them; (c) reports the normalized value of kurtosis, skewness and entropy for each component and in red the threshold.

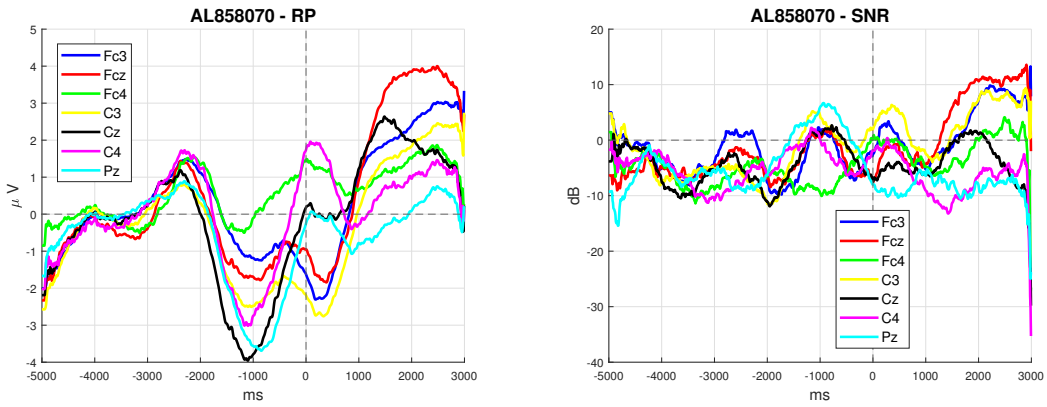

Old Artifact Correction algorithm.

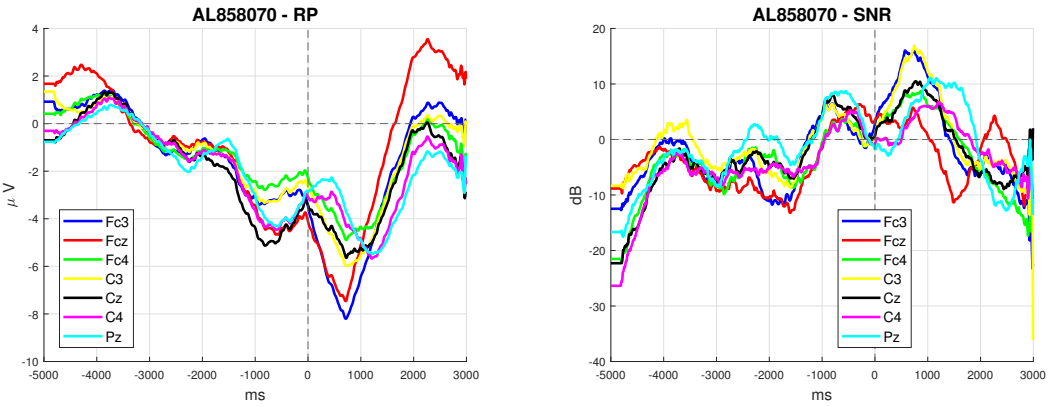

Enhanced Artifact Correction algorithm.

Figure 6.20: AL858070 Semi-voluntary task: RP and SNR obtained with Woody's jitter compensation method.

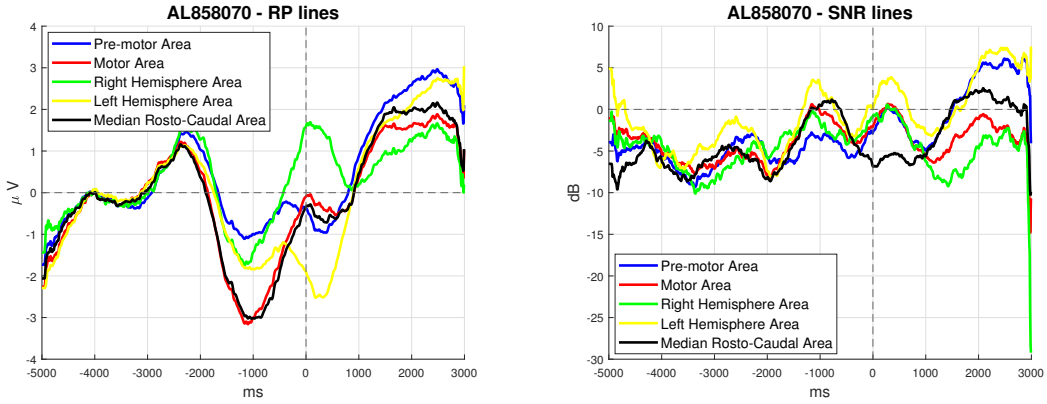

Old Artifact Correction algorithm.

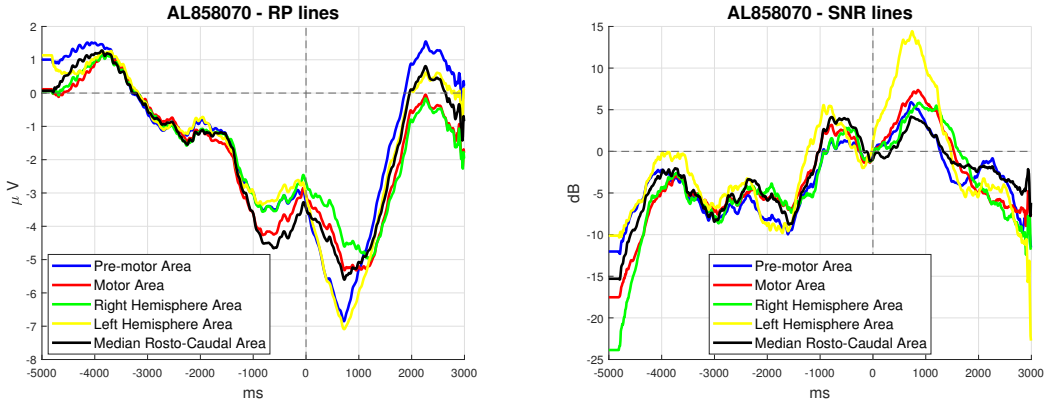

Enhanced Artifact Correction algorithm.

Figure 6.21: AL858070 Semi-voluntary task: RP and SNR of averaged lines obtained with Woody's jitter compensation method.

6.3.3 Involuntary

The involuntary task presents RP with no intention peak and very low or negative SNR.

Dataset FM893061

Artifacts	Previous AC	Enhanced AC
Ocular/EOG	15	2,5
Muscular	3	31
Focal	10,15,23	32
Kurtosis and skewness	All	-
Entropy	All	-

Table 6.6: FM893061 Involuntary task: IC detected and corrected.

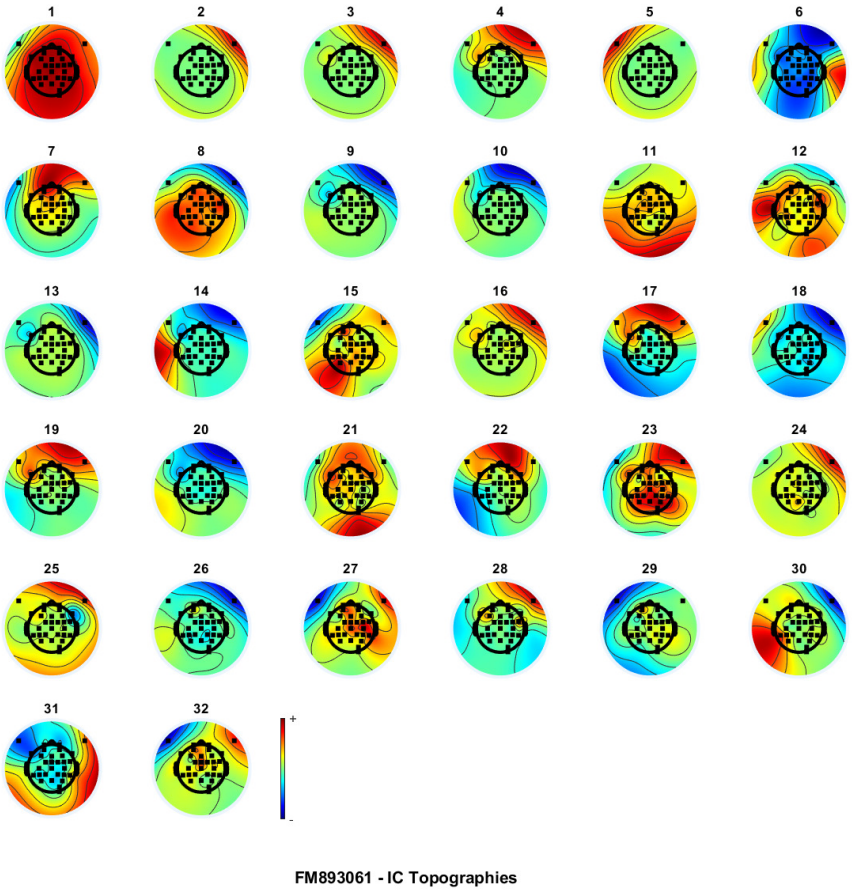

Figure 6.22: FM893061 Voluntary task: Topographies of IC.

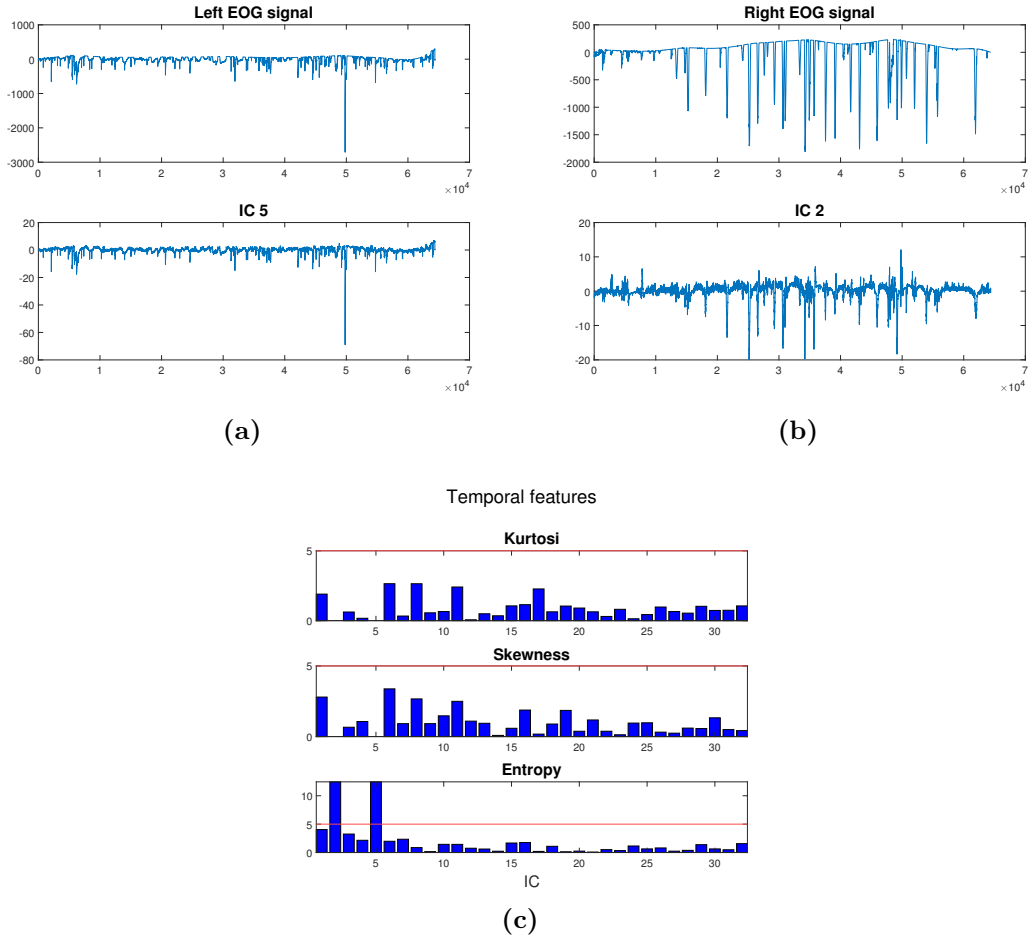

Figure 6.23: FM893061 Involuntary task: (a) and (b) show the EOG signals and the ICs more correlated with them; (c) reports the normalized value of kurtosis, skewness and entropy for each component and in red the threshold.

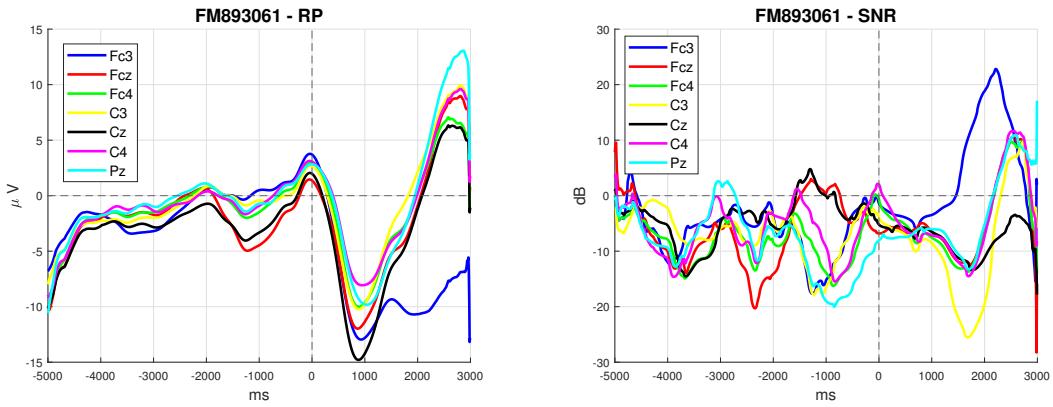

Old Artifact Correction algorithm.

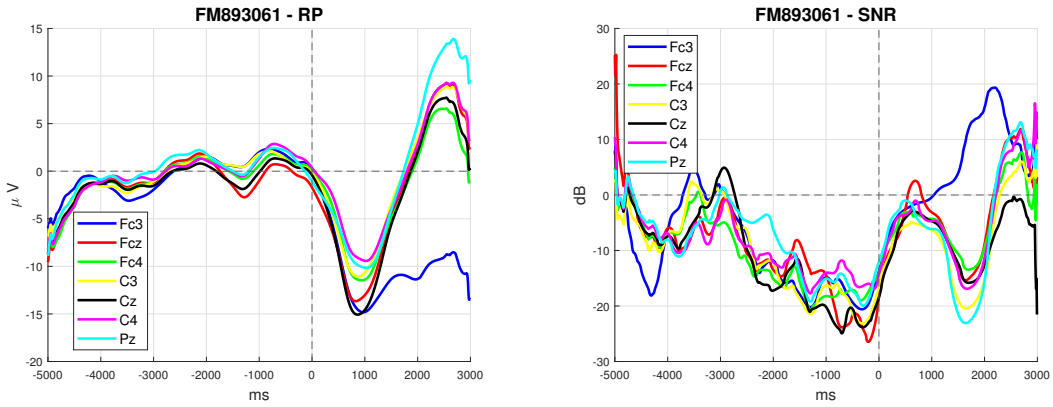

Enhanced Artifact Correction algorithm.

Figure 6.24: FM893061 Involuntary task: RP and SNR obtained with RIDE jitter compensation.

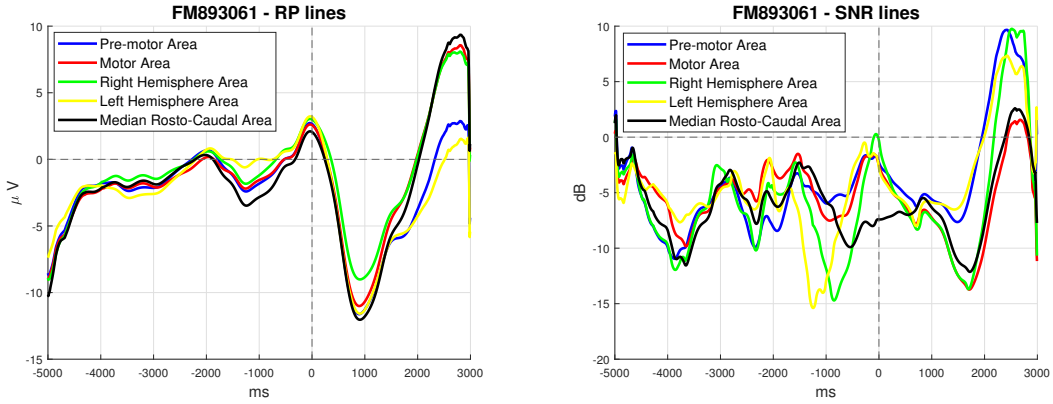

Old Artifact Correction algorithm.

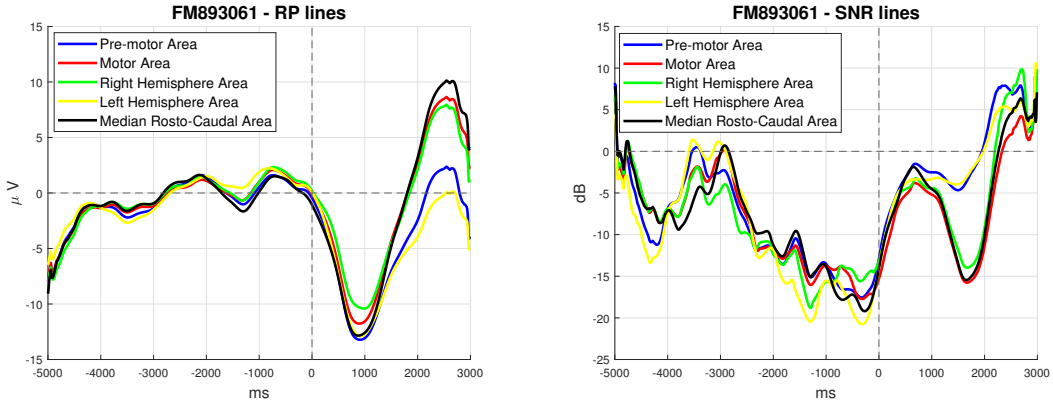

Enhanced Artifact Correction algorithm.

Figure 6.25: FM893061 Involuntary task: RP and SNR of averaged lines obtained with RIDE jitter compensation.

Chapter 7

Slow drifts removal

Slow drifts affecting EEG are due to sweat, which generates skin potentials, or to slight motion of electrodes from their position. These fluctuations can not be suppressed through ICA, but, on the contrary, their effect may be emphasized. High-pass filtering can be a solution, but it raises issues as the removal of slow genuine cortical activity, distortions or spurious deflections. Another technique mostly used is detrending which overcomes the issues caused by filters, but can be applied in different ways. [39]
In this chapter, three types of detrending will be presented and compared.

7.1 Detrending

Detrending means evaluating a smooth function $f(t)$, usually a low order polynomial, best fitting the signal $x(t)$ and then subtracting it from the data:

$$y(t) = x(t) - f(t) \tag{7.1}$$

The scale of fluctuations removed is controlled by the order of the polynomial $f(t)$ which can be estimated by the **least squared method**.

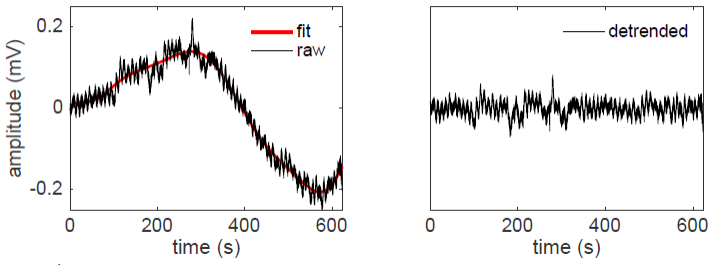

Figure 7.1: Detrending application. On the left, an EEG signal sample (black) and its 10-th order fitting line (red); on the right, the detrended data. Taken from [40]

The main problem of simple detrending is the sensitivity to glitches (due to muscle, motion or electrodes) which affects the function fitting.

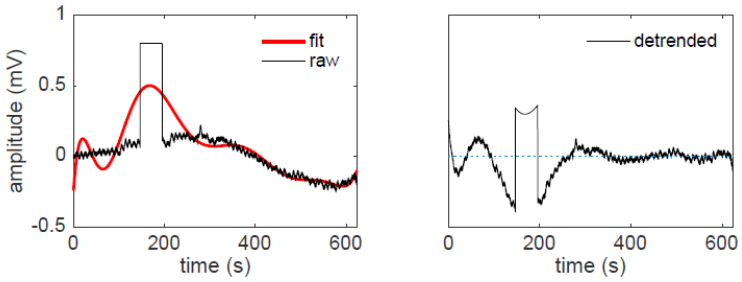

Figure 7.2: Detrending application in presence of a glitch. On the left side, the EEG signal (black) is affected by a glitch that is considered when the fitting line (red) is evaluated; consequently subtracting the fitting line brings a distortion as shown on the right. Taken from [40]

7.2 Robust detrending

Robust detrending tries to overcome the sensitivity to glitches restricting the fit to the intact part of the signal. It is used a **weighted least square** method to evaluate the best fitting line and the weights can be given as a matrix or estimated with a threshold (1).[40]

Algorithm 1 Robust detrending algorithm.

Require: EEG signal $x(t)$
Ensure: detrended EEG $y(t)$, outlier map $w(t)$
  Initialize $w(t) \leftarrow 1$
  while not finished **do**
    $f(t) \leftarrow x(t)$ fit to basis functions using weights$w(t)$
    $d(t) \leftarrow |x(t) - f(t)|$
    if $|d(t)|/STD(|d(t)|) > threshold$ **then**
      $w(t) \leftarrow 0$
    else
      $w(t) \leftarrow 1$
    end if
  end while

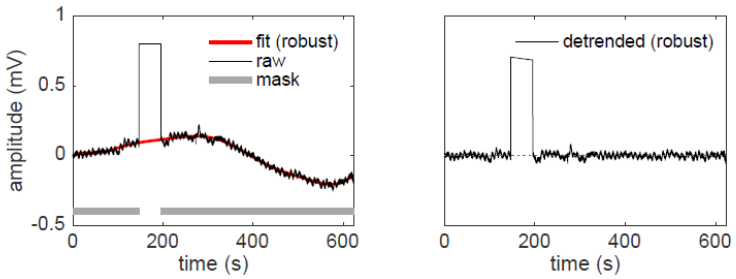

Figure 7.3: Robust Detrending application in presence of a glitch. On the left, an EEG signal sample (black) affected by a glitch and its fitting polynomial (red); on the right, the detrended data. Confronting with Figure 7.2, the fitting line does not consider the glitch and subtraction does not introduce deformations. The grey line indicates that the weights matrix is 0 for the glitch duration.Taken from [40]

However, the weak nature of ERP does not guarantee the masking out of cognitive events of interest. In facts, robust detrending can affect negatively the data for two reasons:

- the polynomial may fit weak but real ERP and subtract them,
- the partial fitting to the peak of an ERP may cause deviation from the baseline activity with displaced and reversed patterns.[39]

7.3 Masked-trial robust detrending

Joram van Driel, Christian N.L. Olivers and Johannes J. Fahrenfort extended robust detrending method to overcome its issues, by masking out the data considered as relevant events.[39] For a trial of 6 s, they pre and post padded 25 s and evaluated the fitting polynomial with a mask excluding the 6 s.

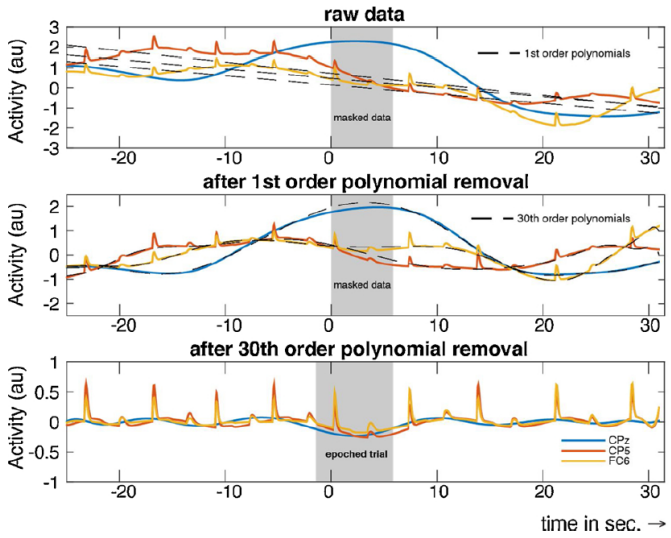

Figure 7.4: Trial-masked Robust Detrending application on data of three electrodes. On the top panel, raw data with the first order the polynomial fits (dotted lines) obtained masking out the trial event(grey panel). In the middle, the data after removing 1st order polynomials fits from the top panel. The dotted lines show the 30th order polynomial fits on these data, from which the trial events were masked out (grey panel in the background). At the bottom, data after removing the 30th order polynomial fits. Finally, the middle trial in grey is segmented out for further analysis. Taken from [39]

7.4 Results

The different methods have been tested on EEG data after interpolation.

- **High-pass filtering.** A 6-order Butterworth filter with cut-off frequency 0.1 Hz was designed with the *butter* Matlab function and applied with *filtfilt* to each EEG channel in order to obtain zero phase distortions.

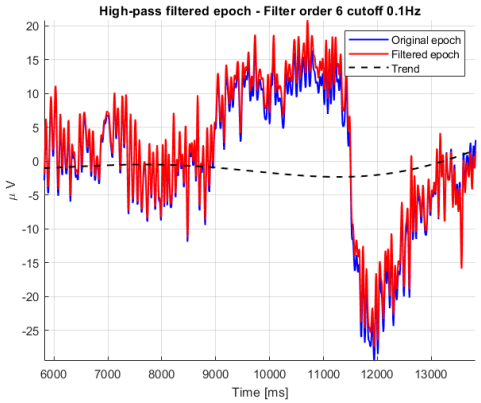

Figure 7.5: Filter effect on an epoch of a single EEG channel.

- **Detrending.** The Matlab function *detrend* has been applied to each channel.

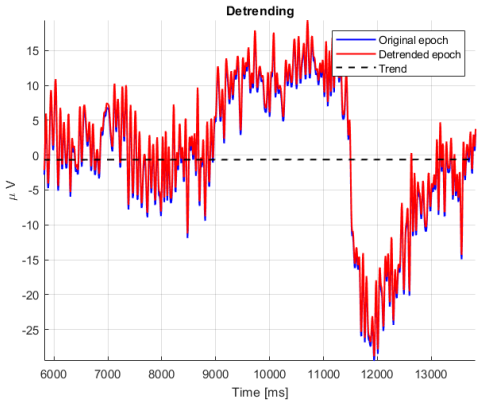

Figure 7.6: Detrending effect on an epoch of a single EEG channel.

- **Robust detrending.** The robust detrending algorithm described in 1 is applied with the function of Noise Tools toolbox *nt_detrend*. The order has been set to 10 after various tests.

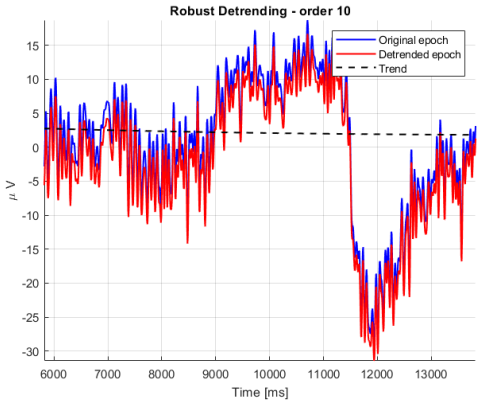

Figure 7.7: Robust detrending effect on an epoch of a single EEG channel.

- **Trial-masked robust detrending.** The *adam_detrend_and_epoch* function in the ADAM toolbox implements the method described above, but, for computational reasons, it has been modified to consider the entire continuous EEG signal masking out the interval of 4 s including the detected onset.

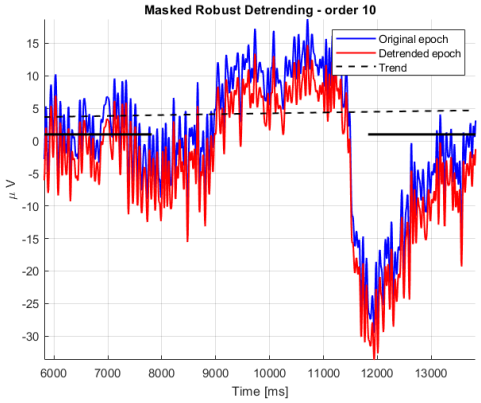

Figure 7.8: Trial-masked robust detrending effect on an epoch of a single EEG channel.

Comparing the methods, there is a slight difference between them, but not enough relevant also in frequency domain. The most concerning consequences are then those reported initially. Consequently, the choice is between robust detrending and trial-masked robust detrending. In the end, the first has been chosen also considering the computational time.

In the following, the RP and SNR of the datasets previously considered are reported here after detrending.

7.4.1 Voluntary

Dataset GF892070

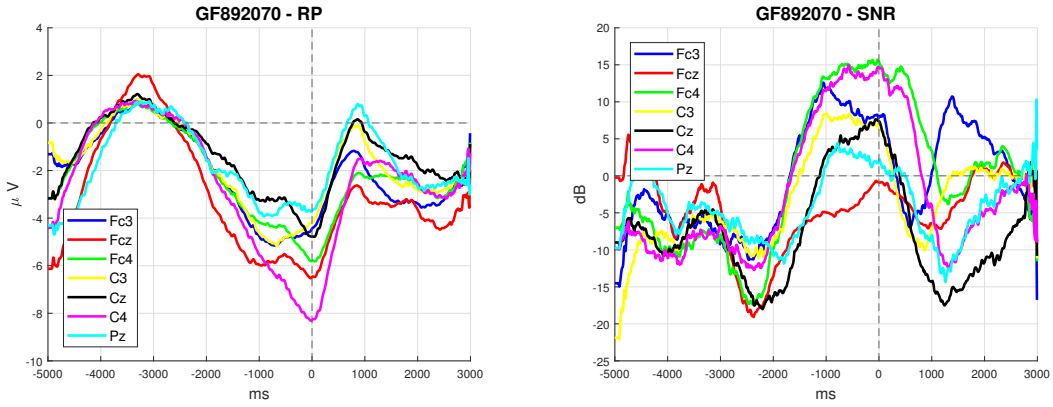

Figure 7.9: GF892070 Voluntary task: RP and SNR obtained with enhanced Artifact Correction algorithm, Robust Detrending and Woody's jitter compensation method.

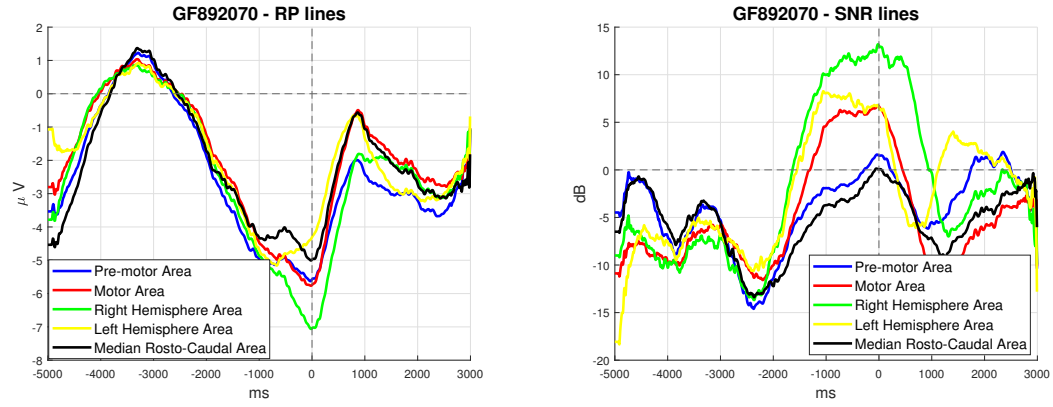

Figure 7.10: GF892070 Voluntary task: RP and SNR of averaged lines obtained with Artifact Correction algorithm, Robust Detrending and Woody's jitter compensation method.

Dataset AL858070

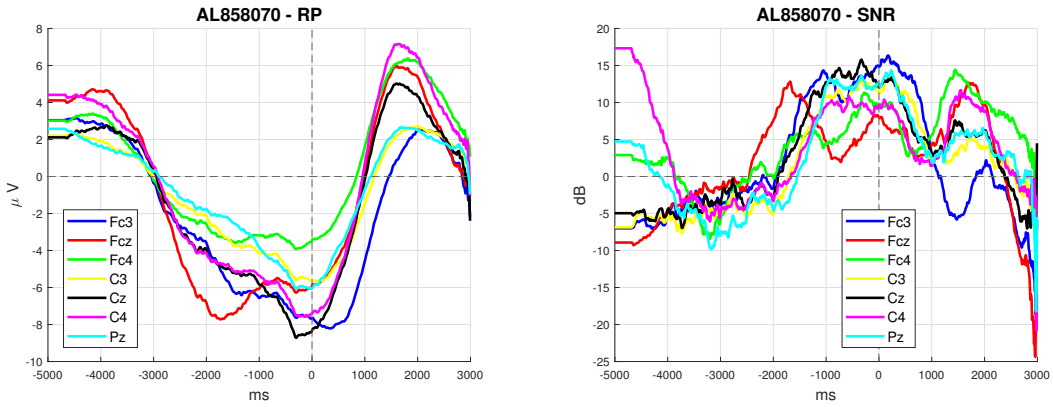

Figure 7.11: AL858070 Voluntary task: RP and SNR obtained with Artifact Correction algorithm, Robust Detrending and Woody's jitter compensation method.

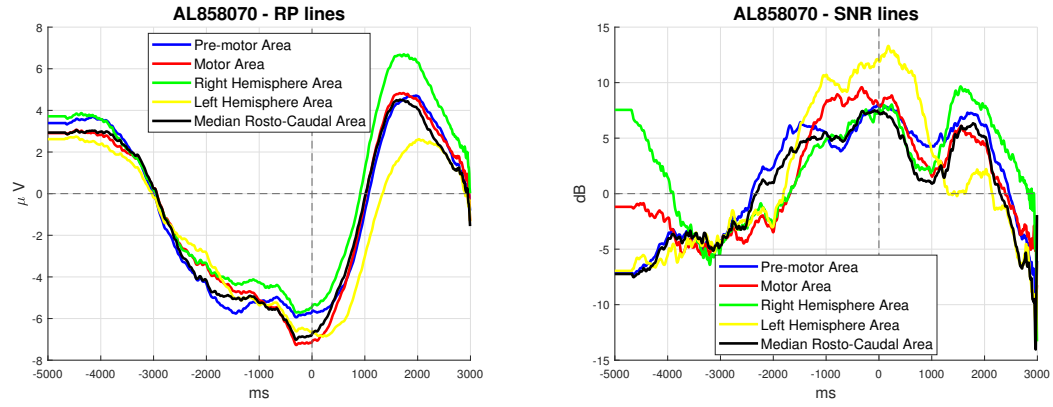

Figure 7.12: AL858070 Voluntary task: RP and SNR of averaged lines obtained with Artifact Correction algorithm, Robust Detrending and Woody's jitter compensation method.

Dataset MI993011

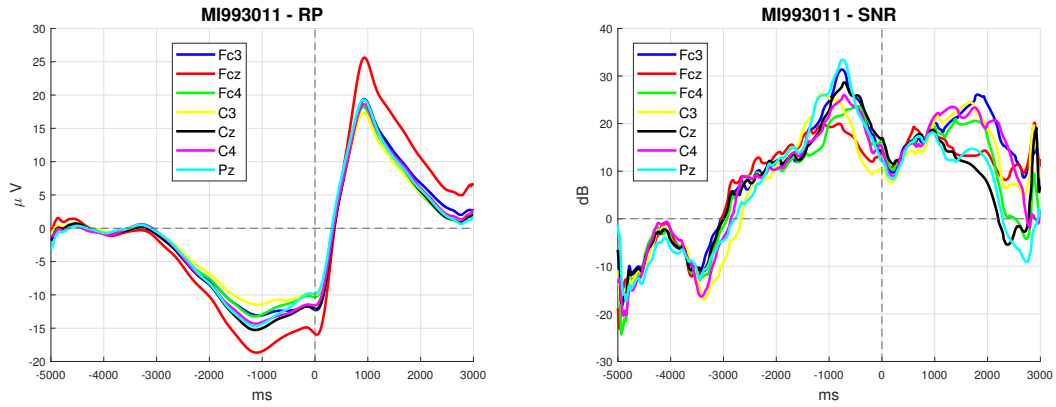

Figure 7.13: MI993011 Voluntary task: RP and SNR obtained with Artifact Correction algorithm, Robust Detrending and RIDE jitter compensation.

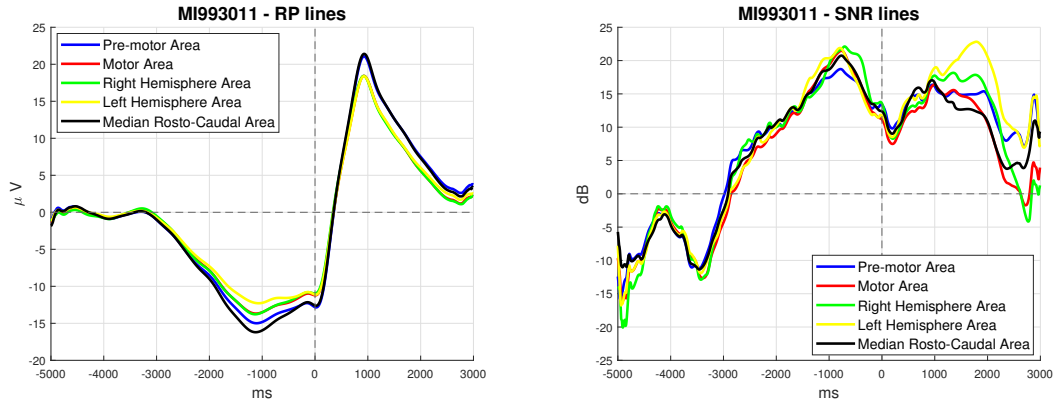

Enhanced Artifact Correction algorithm.

Figure 7.14: MI993011 Voluntary task: RP and SNR of averaged lines obtained with Artifact Correction algorithm, Robust Detrending and RIDE jitter compensation.

Dataset TC995011

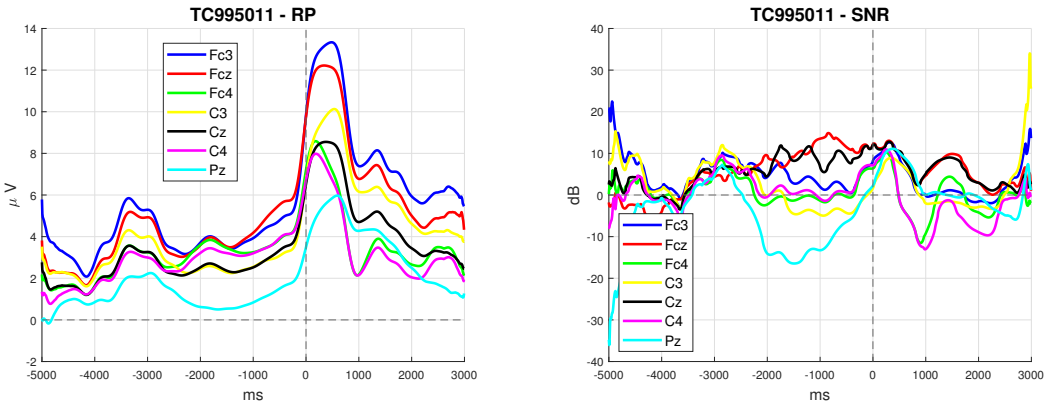

Figure 7.15: TC995011 Voluntary task: RP and SNR obtained with Artifact Correction algorithm, Robust Detrending and RIDE jitter compensation.

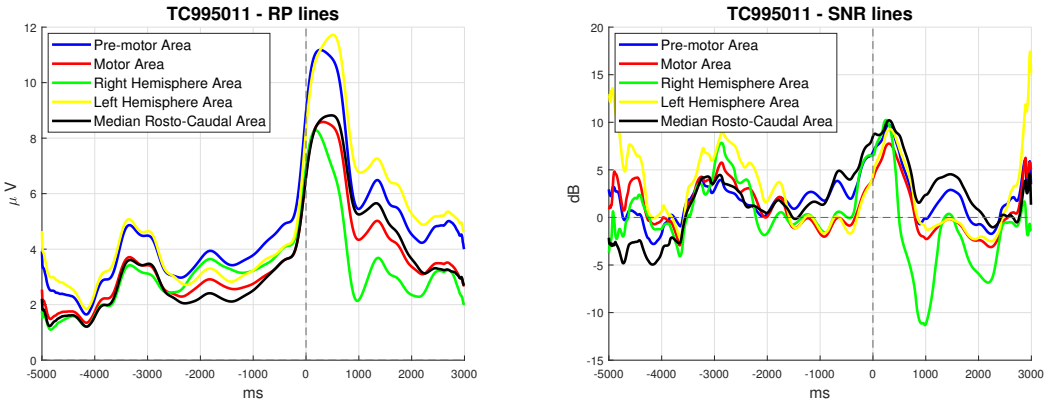

Figure 7.16: TC995011 Voluntary task: RP and SNR of averaged lines obtained with Artifact Correction algorithm, Robust Detrending and RIDE jitter compensation.

7.4.2 Semi-voluntary

Dataset AL858070

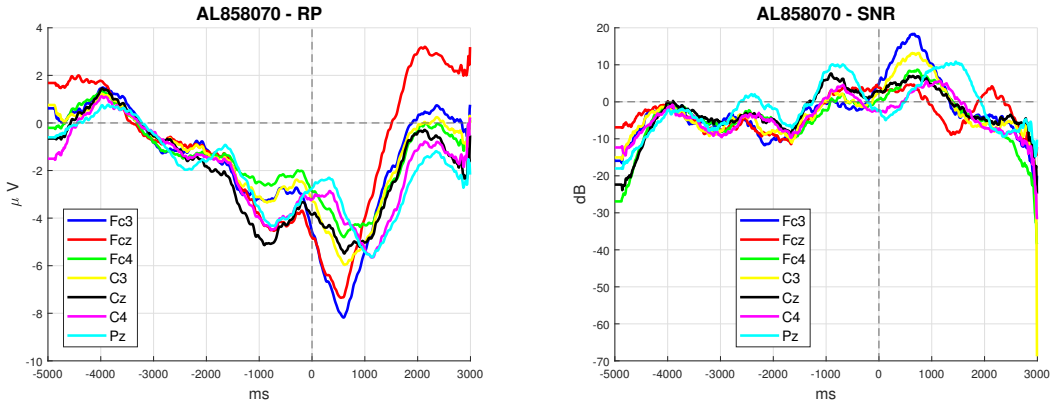

Figure 7.17: AL858070 Semi-voluntary task: RP and SNR obtained with Artifact Correction algorithm, Robust Detrending and Woody's jitter compensation method.

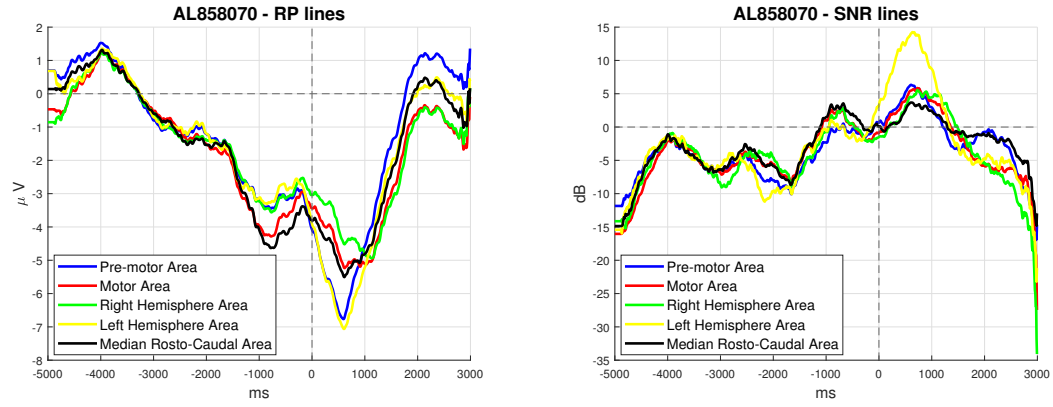

Figure 7.18: AL858070 Semi-voluntary task: RP and SNR of averaged lines obtained with Artifact Correction algorithm, Robust Detrending and Woody's jitter compensation method.

7.4.3 Involuntary

Dataset FM893061

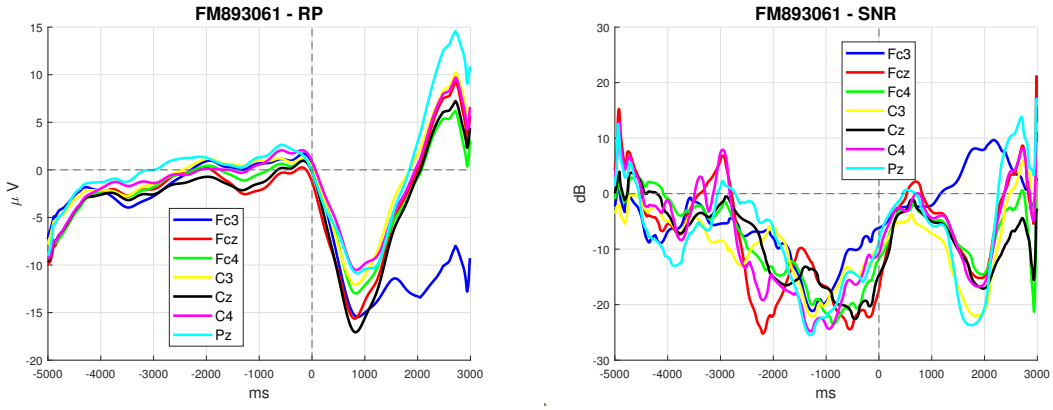

Figure 7.19: FM893061 Involuntary task: RP and SNR obtained with Artifact Correction algorithm, Robust Detrending and RIDE jitter compensation.

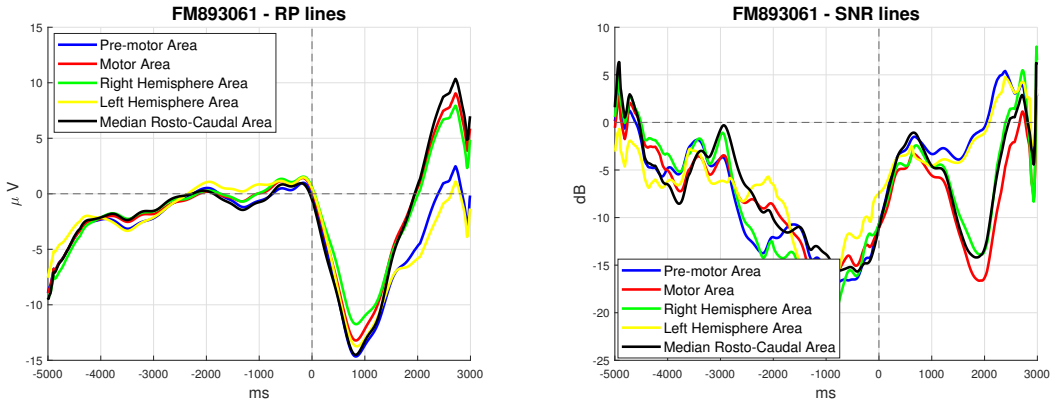

Figure 7.20: FM893061 Involuntary task: RP and SNR of averaged lines obtained with Artifact Correction algorithm, Robust Detrending and RIDE jitter compensation.

Chapter 8

Study on hemiplegic patients

Hemiplegia is the temporary or permanent condition of partial paralysis that patients may experience after brain injuries. The motor response on one side of the body is weak or absent depending on the level of injury.
In this chapter, it is introduced the application of the pre-processing chain on dataset acquired from patients affected by left hemiplegia (i.e. with injured right hemisphere). Patients are asked to perform unimanual and bimanual tasks to prove that motor intention is preserved and stronger on the non-hemiplegic hemisphere. In this case, the recordings use 7 electrodes montage which do not allow a good ICA; moreover, the EMG and EEG signals are noisier than those of healthy subjects, then the pre-processing is done in a slightly different way.

8.1 Pre-Processing

The first step in pre-processing is the identification of movement onsets.
In MRCPLAB, the extraction of onsets exploits two EMG signals: the raw, from the electromyograph, and the TKEO, obtained processing the raw EMG to maximize the SNR. If the Labjack signal is available, it also will contribute.
For patient's datasets, the EMG are noisy and sometimes the onsets are not correctly identified; therefore, the movement onsets are extracted by looking at the peaks of raw EMG for each dataset.
Secondly, the raw EEG is analysed to find artifacts: if a large peak affects all the channels or it is temporally close to an onset, then the time onset is deleted and not considered in epoching.
Then, different techniques are applied to clean the EEG signals:

- **Kalman filter**, it is widely used in signal processing to remove Gaussian noise and, in this case, it is applied with Autoregressive model of order 6;

- **Peak correction**, used to correct peaks not too close to the onset, it sets to zero or interpolate samples larger than a given threshold ($\sim 10\,\mu V - 20\,\mu V$);

- **Robust detrending**, as previously described, it is used to correct slow drifts.

Depending on the dataset, these methods are used jointly or not used.
Successively, epoching and baseline correction are applied. Before averaging, it is possible to compensate jitter with Woody's method aligning all epochs to Fcz channel.

8.2 Results

The bimanual task implies the intention of moving both hands and then a small difference between Fc3 and Fc4 in the time interval $-1\,s$ to $0\,s$; while for the unimanual task, intention (and movement) should be predominant in Fc3 (the experiment involved the movement of the right finger and then the activation of left hemisphere).
The results from the dataset MC373010 (8.1) and DV373010 (8.2) show what described above: Fc3 is very close to Fc4 in the bimanual task; Fc3 is greater than Fc4 in the unimanual.

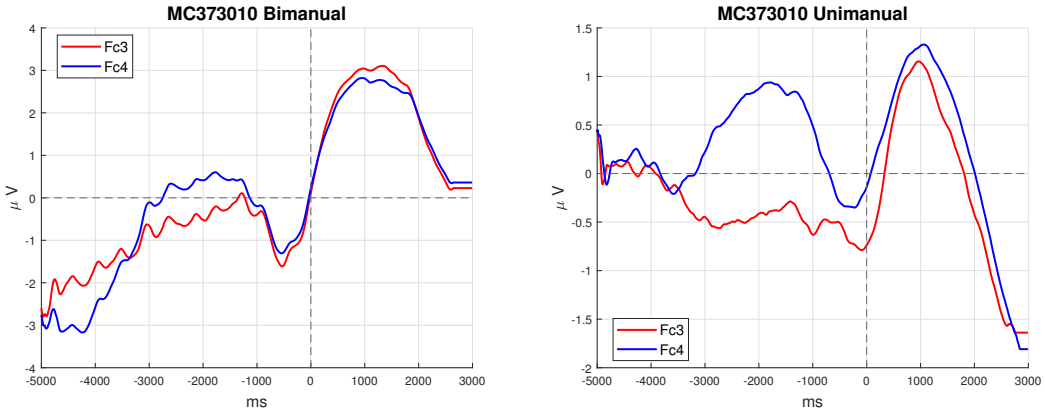

(a) **(b)**

Figure 8.1: Hemiplegic MC373010 results: the bimanual task (a) shows a small difference between Fc3 and Fc4 in the time interval $-1\,s$–$0\,s$; on the contrary, the unimanual task (b) shows a larger difference.

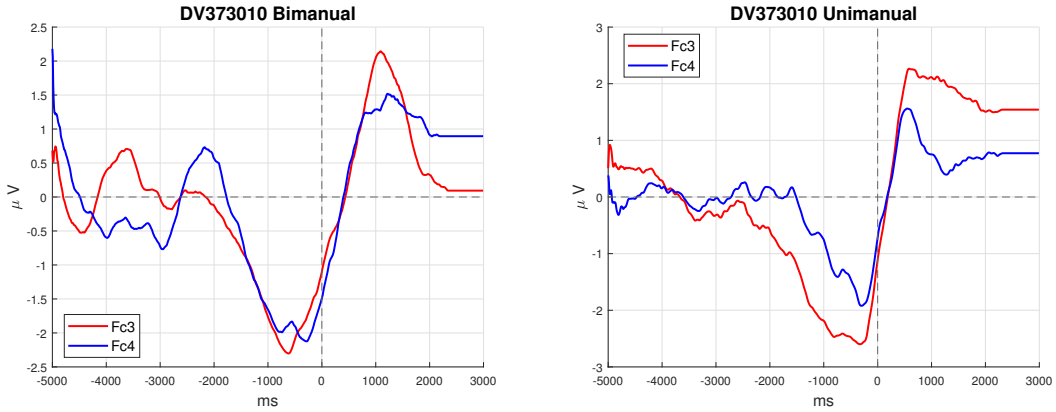

(a) **(b)**

Figure 8.2: Hemiplegic DV373010 results: the bimanual task (a) shows a small difference between Fc3 and Fc4 in the time interval −1 s–0 s; on the contrary, the unimanual task (b) shows a larger difference.

The Fc3 signal in the bimanual task of the subject FR351070 (8.3) is smaller than Fc4, which means that the intention on the right hemisphere requires a lot of effort for the patient.

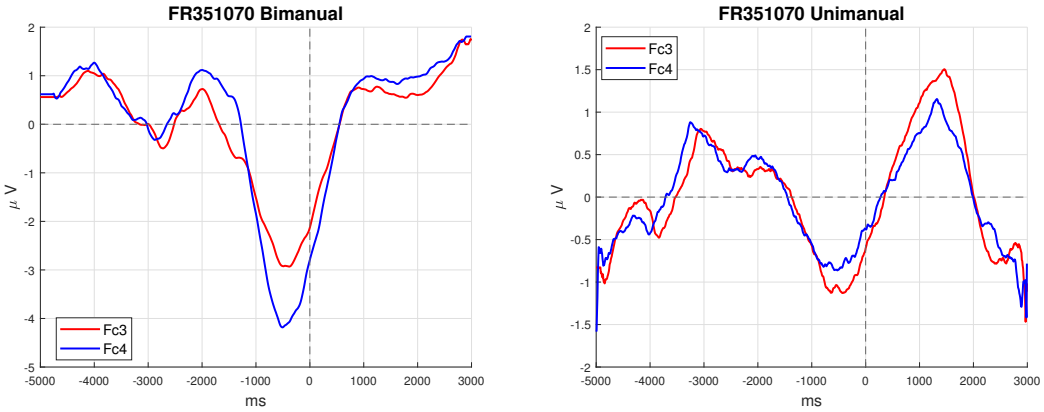

(a) **(b)**

Figure 8.3: Hemiplegic FR351070 results: the bimanual task (a) shows greater value of Fc4 in −1 s–0 s since it requires a lot of effort for the patient; the unimanual (b) has Fc3 values larger than Fc4.

The recordings of two more subjects were analysed, but the noisy recording of one task did not allow a paired comparison. However, the bimanual task of

AI390071 (8.4) confirms the smaller difference between Fc3 and Fc4; the RP of unimanual task of AC390060 (8.5) has larger values of Fc3 w.r.t. Fc4 in the considered time interval.

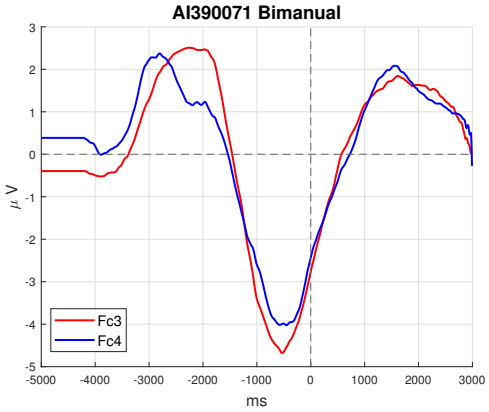

Figure 8.4: Hemiplegic AI390071 result: the bimanual task has a small difference between Fc3 and Fc4.

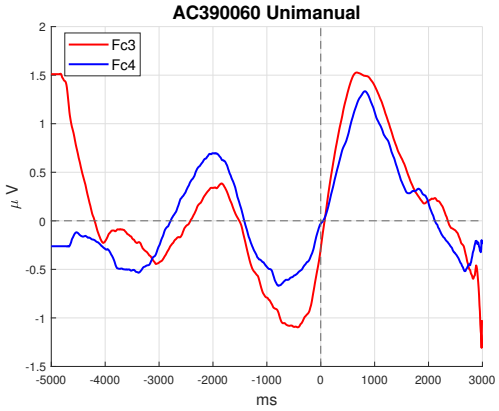

Figure 8.5: Hemiplegic AC390060 result: the unimanual task has a larger difference between Fc3 and Fc4.

Finally, to confirm the graphic results, the RMS Powers of Fc3 and Fc4 in $-1\,\mathrm{s}$–$0\,\mathrm{s}$, and their differences were evaluated for each dataset and reported in 8.1, 8.2 and 8.3.

Dataset	Bimanual task		
	$P_{RMS}\|_{Fc3}$	$P_{RMS}\|_{Fc4}$	$P_{RMS}\|_{Fc3} - P_{RMS}\|_{Fc4}$
MC373010	1.7381	1.4183	0.31987
DV373010	2.0796	2.0042	0.075316
FR351070	2.7942	4.0226	-1.2284
AI390071	4.3392	3.8438	0.49538
AC390060	–	–	–

Table 8.1: RMS powers [µV] in the time interval −1 s–0 s

Dataset	Unimanual task		
	$P_{RMS}\|_{Fc3}$	$P_{RMS}\|_{Fc4}$	$P_{RMS}\|_{Fc3} - P_{RMS}\|_{Fc4}$
MC373010	0.95755	0.44591	0.51164
DV373010	2.5617	1.7201	0.84161
FR351070	1.2104	1.0114	0.19892
AI390071	–	–	–
AC390060	1.0697	0.67532	0.39438

Table 8.2: RMS powers [µV] in the time interval −1 s–0 s

$P_{RMS}\|_{Fc3} - P_{RMS}\|_{Fc4}$		
Dataset	Unimanual	Bimanual
MC373010	0.51164	0.31987
DV373010	0.84161	0.075316
FR351070	0.19892	-1.2284
AI390071	–	0.49538
AC390060	0.39438	–

Table 8.3: RMS powers [µV] in the time interval −1 s–0 s

Chapter 9

Conclusions

This thesis focuses on improving the pre-processing chain, in particular the automated Artifact Correction and the detrending algorithms, to obtain Readiness Potentials with higher quality allowing a more accurate classification. Moreover, it is proposed the application of the pre-processing chain to datasets obtained from hemiplegic patients.

Artifact correction enhancements allowed the objective detection of artifacts exploiting frequency and statistical features of Independent Components. It allowed improvements to the Signal-to-Noise Ratio and the shape of RPs. The limitations of the algorithm are given by the Independent Components Analysis which require an sufficient number of channels to adequately separate components. Therefore, testing the algorithm with a larger number of channels may allow to study whether more improvements may be applied to detect and correct other type of artifacts.

The detrending implementation does not produce visible improvements, but it does not affect the RPs negatively. Therefore, including it in the pipeline will not worsen the signal or introduce distortions.

Finally, the application of pre-processing to hemiplegic patients' dataset allows to study of Lateralized Readiness Potential and its features. The analysis of more datasets can increase the statistical validity of the results.

Summarizing, more improvements in the pre-processing chain will certainly allow a better classification of the motor tasks, but, more importantly, it will allow the recognition of minimal state of consciousness and it will give more information about the state of patients whose awareness cannot be easily proved.

Bibliography

[1] Don E. Marietta. «Conscience in Greek Stoicism». In: *Numen* 17.3 (1970), pp. 176–187. ISSN: 002959732. URL: http://www.jstor.org/stable/3269701 (visited on 12/20/2022) (cit. on p. 1).

[2] Rocco J. Gennaro. *Consciousness*. The Internet Encyclopedia of Philosophy, ISSN 2161-0002. 2022. URL: https://iep.utm.edu/consciousness (cit. on p. 1).

[3] Cambridge University Press, ed. *Consciousness*. 2022. URL: https://dictionary.cambridge.org/dictionary/english/consciousness (cit. on p. 1).

[4] Christof Koch. «What is consciousness?» In: *Nature* 557 (May 2018), S8–S12. DOI: https://doi.org/10.1038/d41586-018-05097-x (cit. on pp. 2–4).

[5] Mario Manfredi. *La coscienza e i suoi fondamenti biologici*. Treccani. 2010. URL: https://www.treccani.it/enciclopedia/la-coscienza-e-i-suoi-fondamenti-biologici_%28XXI-Secolo%29/ (cit. on p. 3).

[6] Giulio Tononi et al. «Consciousness and Complexity». In: *Science* 282 (Dec. 1998), pp. 1846–1851. DOI: 10.1126/science.282.5395.1846 (cit. on p. 3).

[7] Minji Lee, Leandro R. D. Sanz, Alice Barra, et al. «Quantifying arousal and awareness in altered states of consciousness using interpretable deep learning.» In: *Nature Communications* 13, 1064 (2022). DOI: https://doi.org/10.1038/s41467-022-28451-0 (cit. on p. 4).

[8] Andrea Nani, Jordi Manuello, Lorenzo Mancuso, Donato Liloia, Tommaso Costa, and Franco Cauda. «The Neural Correlates of Consciousness and Attention: Two Sister Processes of the Brain.» In: *Frontiers in Neuroscience* 13.1169 (2019). DOI: https://doi.org/10.3389/fnins.2019.01169 (cit. on p. 5).

[9] Camille Chatelle and Steven Laureys. «Understanding Disorders of Consciousness». In: *Oxford Handbook of Neuroethics* (Jan. 2012). DOI: 10.1093/oxfordhb/9780199570706.013.0037 (cit. on p. 6).

[10] Heinrich Binder. «Clinical Evaluation of Residual Brain Function and Responsiveness in Disorders of Consciousness». In: *Brain Function and Responsiveness in Disorders of Consciousness*. Ed. by Springer International Publishing Switzerland. 2016. DOI: 10.1007/978-3-319-21425-2_4 (cit. on p. 6).

[11] Gianluigi Gigli, Antonio Carolei, Paolo Maria Rossini, and Rachele Zylberman. *Stato Vegetativo e di Minima Coscienza*. Ministero della Salute, Dec. 2009 (cit. on p. 6).

[12] Johns Hopkins Medicine. *Brain Anatomy and How the Brain Works*. 2023. URL: https://www.hopkinsmedicine.org/health/conditions-and-diseases/anatomy-of-the-brain (cit. on pp. 7–9).

[13] American Association of Neurological Surgeons. *Anatomy of the Brain*. 2023. URL: https://www.aans.org/en/Patients/Neurosurgical-Conditions-and-Treatments/Anatomy-of-the-Brain (cit. on pp. 7, 9, 10).

[14] Cherry Kendra. *Parts of the Brain*. 2022. URL: https://www.verywellmind.com/the-anatomy-of-the-brain-2794895 (cit. on p. 9).

[15] Tonya Hines. *Anatomy of the Brain*. Mayfield Clinic. 2018. URL: https://mayfieldclinic.com/pe-anatbrain.htm#:~:text=The%20brain%20has%20three%20main,and%20fine%20control%20of%20movement. (cit. on pp. 9–11).

[16] Visible body. *The Human Brain: Anatomy and Function*. 2023. URL: https://www.visiblebody.com/learn/nervous/brain (cit. on p. 9).

[17] Neuroscienze. *I Neuroni e le Cellule Gliali*. 2010. URL: https://www.neuroscienze.net/i-neuroni-e-le-cellule-gliali/ (cit. on p. 11).

[18] Molecular Devices. *What is an action potential?* 2023. URL: https://www.moleculardevices.com/applications/patch-clamp-electrophysiology/what-action-potentialttps://www.visiblebody.com/learn/nervous/brain (cit. on p. 11).

[19] Lecturio. *Synapses and Neurotransmission*. 2023. URL: https://www.lecturio.com/concepts/synapses-and-neurotransmission/ (cit. on p. 12).

[20] Steven J. Luck. *An introduction to the event-related potential technique*. The MIT Press, 2014. ISBN: 978-0-262-52585-5 (cit. on pp. 12, 13, 29–33, 35, 40, 41).

[21] Patrick Haggard. «Conscious Intention and Motor Cognition». In: *Cognitive Science* 9.6 (June 2005), pp. 290–295. DOI: https://doi-org.ezproxy.biblio.polito.it/10.1016/j.tics.2005.04.012 (cit. on pp. 15, 21).

[22] R.C. Miall and D.M. Wolpert. «Forward Models for Physiological Motor Control». In: *Neural Networks* 9.8 (Nov. 1996), pp. 1265–1279. DOI: https://doi-org.ezproxy.biblio.polito.it/10.1016/S0893-6080(96)00035-4 (cit. on p. 15).

[23] Roberta Schifano. «Experimental evidences of the presence of the motor intention and the motor planning in person suffering from brain damage using Lateralized Readiness Potentials». M. Eng. thesis. Università degli stuti di Padova, 2012 (cit. on p. 16).

[24] Gonzalo M. Rojas, Carolina Alvarez, Carlos E. Montoya, María de la Iglesia-Vayá, Jaime E. Cisternas, and Marcelo Galvez. «Study of Resting-State Functional Connectivity Networks Using EEG Electrodes Position As Seed». In: *Frontiers in Neuroscience* 12 (Apr. 2018). ISSN: 1662-453X. DOI: 10.3389/fnins.2018.00235. URL: https://www.frontiersin.org/articles/10.3389/fnins.2018.00235 (cit. on p. 17).

[25] D. Purves, G.J Augustine, D. Fitzpatrick, et al. «The Motor Unit». In: *Neuroscience*. Sunderland (MA): Sinauer Associates, 2001. URL: https://www.ncbi.nlm.nih.gov/books/NBK10874/ (cit. on p. 18).

[26] Shravani Sur and VK Sinha. «Event-related potential: An overview.» In: *Ind Psychiatry J.* 18(1) (Jan. 2009), pp. 70–3. DOI: 10.4103/0972-6748.57865 (cit. on p. 19).

[27] Aaron Schurger, Pengbo 'Ben' Hu, Joanna Pak, and Adina L. Roskies. «What is the Readiness Potential?» In: *Trends in Cognitive Sciences* 25.7 (July 2021), pp. 558–70. DOI: https://doi.org/10.1016/j.tics.2021.04.001 (cit. on p. 19).

[28] Chiara Botrugno. «Enhancement of Readiness Potentials' Pre-Processing Chain in an Brain-Computer Interface for nonresponsive patients». M. Eng. thesis. Politecnico di Torino, July 2022 (cit. on p. 19).

[29] Cornelia Kranczioch, Simon Mathews, Phil J.A. Dean, and Annette Sterr. «On the Equivalence of Executed and Imagined Movements: Evidence from Lateralized Motor and Nonmotor Potentials». In: *Human Brain Mapping* 30.10 (Oct. 2009), pp. 3275–3286. DOI: 10.1002/hbm.20748 (cit. on p. 20).

[30] Patrick Haggard. «Human volition: towards a neuroscience of will». In: *Nature Reviews Neuroscience* 9.6 (Dec. 2008), pp. 934–946. DOI: 10.1038/nrn2497 (cit. on p. 21).

[31] Benjamin Libet, W.W. Elwood, and A.G. Curtis. «Readiness-potentials preceding unrestricted 'spontaneous' vs. pre-planned voluntary acts». In: *Electroencephalography and Clinical Neurophysiology* 54.3 (Sept. 1982), pp. 322–335. DOI: https://doi.org/10.1016/0013-4694(82)90181-X (cit. on p. 21).

[32] Bit Brain Team. *All about EEG artifacts and filtering tools*. 2020. URL: https://www.bitbrain.com/blog/eeg-artifacts (cit. on p. 29).

[33] David Valentine. *Artifacts*. 2020. URL: https://www.learningeeg.com/artifacts (cit. on pp. 29, 31–38).

[34] Swartz Center for Computational Neuroscience. *ICLabel Tutorial: EEG Independent Component Labeling*. URL: https://labeling.ucsd.edu/tutorial/labels (cit. on pp. 33, 35, 36).

[35] Scott Makeig and Julie Onton. «ERP features and EEG dynamics: An ICA perspective». In: *The Oxford Handbook of Event-Related Potential Components* (Jan. 2012). DOI: 10.1093/oxfordhb/9780195374148.013.0035 (cit. on pp. 40, 41).

[36] Anthony J. Bell and Terrence J. Sejnowski. «An information-maximisation approach to blind separation and blind deconvolution.» In: *Neural Computation* 7(6) (Nov. 1995), pp. 1129–59. DOI: 10.1162/neco.1995.7.6.1129 (cit. on p. 42).

[37] Irene Winkler, Stefan Haufe, and Michael Tangermann. «Automatica classification of artifactual ICA-components for artifact removal in EEG signals.» In: *Behavioural and Brain Functions* 2 (Aug. 2011), pp. 7–30. DOI: 10.1186/1744-9081-7-30 (cit. on p. 43).

[38] Margherita Urso. «Sviluppo di un metodo per la rimozione automatica e manuale degli artefatti per una BCI per pazienti non responsivi». M. Eng. thesis. Politecnico di Torino, Oct. 2021 (cit. on p. 43).

[39] Joram van Driel, Christian N.L. Olivers, and Joannes J. Fahrenfort. «High-pass filtering artifacts in multivariate classification of neural time series data.» In: *Journal of Neuroscience Methods* 352 (Jan. 2021), p. 109080. ISSN: 0165-0270. DOI: https://doi.org/10.1016/j.jneumeth.2021.109080. URL: https://www.sciencedirect.com/science/article/pii/S0165027021000157 (cit. on pp. 70, 72, 73).

[40] Alain de Cheveigné and Dorothée Arzounian. «Robust detrending, rereferencing, outlier detection, and inpainting for multichannel data.» In: *NeuroImage* 172 (Feb. 2018), pp. 903–912. ISSN: 1053-8119. DOI: https://doi.org/10.1016/j.neuroimage.2018.01.035. URL: https://www.sciencedirect.com/science/article/pii/S1053811918300351 (cit. on pp. 71, 72).